

University of Windsor

## Scholarship at UWindor

---

Electronic Theses and Dissertations

Theses, Dissertations, and Major Papers

---

1-24-2019

# Storage Impacts and Biogeochemical Characterization of Acid Mine Drainage Sludge from a Novel Mussel Shell Bioreactor

Sara Butler

*University of Windsor*

Follow this and additional works at: <https://scholar.uwindsor.ca/etd>

---

### Recommended Citation

Butler, Sara, "Storage Impacts and Biogeochemical Characterization of Acid Mine Drainage Sludge from a Novel Mussel Shell Bioreactor" (2019). *Electronic Theses and Dissertations*. 7632.

<https://scholar.uwindsor.ca/etd/7632>

This online database contains the full-text of PhD dissertations and Masters' theses of University of Windsor students from 1954 forward. These documents are made available for personal study and research purposes only, in accordance with the Canadian Copyright Act and the Creative Commons license—CC BY-NC-ND (Attribution, Non-Commercial, No Derivative Works). Under this license, works must always be attributed to the copyright holder (original author), cannot be used for any commercial purposes, and may not be altered. Any other use would require the permission of the copyright holder. Students may inquire about withdrawing their dissertation and/or thesis from this database. For additional inquiries, please contact the repository administrator via email ([scholarship@uwindsor.ca](mailto:scholarship@uwindsor.ca)) or by telephone at 519-253-3000ext. 3208.

**Storage Impacts and Biogeochemical Characterization of Acid Mine  
Drainage Sludge from a Novel Mussel Shell Bioreactor**

By

**Sara Butler**

A Thesis  
Submitted to the Faculty of Graduate Studies  
through the Great Lakes Institute for Environmental Research  
in Partial Fulfillment of the Requirements for  
the Degree of Master of Science  
at the University of Windsor

Windsor, Ontario, Canada

2019

© 2019 Sara Butler

**Storage Impacts and Biogeochemical Characterization of Acid Mine  
Drainage Sludge from a Novel Mussel Shell Bioreactor**

by

**Sara Butler**

APPROVED BY:

---

C. Semeniuk

Department of Biological Sciences

---

J. Pope

Great Lakes Institute for Environmental Research

---

D. Heath, Co-Advisor

Great Lakes Institute for Environmental Research

---

C. Weisener, Advisor

Great Lakes Institute for Environmental Research

January 14, 2019

## **DECLARATION OF CO-AUTHORSHIP / PREVIOUS PUBLICATION**

### **i. Co-Authorship**

I hereby declare that this thesis incorporates material that is result of joint research, as follows: Chapter 2 of the thesis was coauthored with Dr. James Pope and Dr. Subba Rao Chaganti, under the supervision of Dr. Daniel D. Heath and Dr. Christopher G. Weisener. The primary contributions, data analysis, interpretation, and writing were performed by the author. Co-authors contributed by contributing to editing of manuscript, statistical analysis, and project conceptualization.

I am aware of the University of Windsor Senate Policy on Authorship and I certify that I have properly acknowledged the contribution of other researchers to my thesis, and have obtained written permission from each of the co-author(s) to include the above material(s) in my thesis.

I certify that, with the above qualification, this thesis, and the research to which it refers, is the product of my own work.

### **ii. Previous Publication**

This thesis includes one original paper that have been previously published/submitted for publication in peer reviewed journals, as follows:

Thesis Chapter	Publication title/full citation	Publication status*
<i>Chapter 2</i>	<i>Butler S, Pope J, Chaganti S, et al (2019) Biogeochemical Characterization of Metal Behavior from Novel Mussel Shell Bioreactor Sludge Residues. Geosciences 9:50. doi: 10.3390/geosciences9010050</i>	<i>Published in Geosciences (MDPI)</i>

I certify that I have obtained a written permission from the copyright owner(s) to include the above published material(s) in my thesis. I certify that the above material describes work completed during my registration as a graduate student at the University of Windsor.

### iii. General

I declare that, to the best of my knowledge, my thesis does not infringe upon anyone's copyright nor violate any proprietary rights and that any ideas, techniques, quotations, or any other material from the work of other people included in my thesis, published or otherwise, are fully acknowledged in accordance with the standard referencing practices. Furthermore, to the extent that I have included copyrighted material that surpasses the bounds of fair dealing within the meaning of the Canada Copyright Act, I certify that I have obtained a written permission from the copyright owner(s) to include such material(s) in my thesis.

I declare that this is a true copy of my thesis, including any final revisions, as approved by my thesis committee and the Graduate Studies office, and that this thesis has not been submitted for a higher degree to any other University or Institution.

## **ABSTRACT**

Acid mine drainage (AMD) remediation commonly produces by products which must be stored or utilized to reduce the risk of further contamination. A mussel shell bioreactor has been implemented at a coal mine in New Zealand, which is an effective remediation option, even though an accumulated sludge layer decreased efficiency. To understand associated risks related to storage or utilizing the AMD sludge material, a laboratory mesocosm study investigated the physio-chemical and biological influences under two conditions: anoxic storage (burial deep within a waste rock dump) and exposure to oxic environments (use of sludge on the surface of the mine). Solid phase characterization by SEM (scanning electron microscope) and selective extraction was completed to compare two environmental conditions (oxic and anoxic) under biologically active and abiotic systems (achieved by gamma irradiation). Changes in microbial community structure were monitored using 16s rDNA amplification and next-generation sequencing. The results indicate that microbes in an oxic environment increase the formation of oxyhydroxides and acidic conditions increase metal mobility. In an oxic and circumneutral environment, the AMD sludge may be repurposed to act as an oxygen barrier for mine tailings or soil amendment. Anoxic conditions would likely promote the biomineralization of sulfide minerals in the AMD sludge by sulfate reducing bacteria (SRB) which were abundant in the system. The anoxic conditions reduced the risk of contaminants from oxides but increased the risk of Fe associated with organic material. In summary, fewer risks are associated with anoxic burial but repurposing in an oxic condition may be appropriate under favorable conditions such as a neutral pH.

## DEDICATION

*This thesis is dedicated to my parents, Bev and Chuck Butler, for their constant love and support. Thank-you for the encouragement and sacrifices that made my education possible.*

## **ACKNOWLEDGEMENTS**

This research was funded in part by grants from the Natural Sciences and Engineering Council of Canada (NSERC) Discovery program 860006, ERASMUS CREATE grant 397997-2011, MITACS, and IT08566 Global Partnership Award funding provided by Bathurst Resources, O’Kane Consulting and New Zealand MBIE research contract 1403 held by CRL energy.

I would like to thank my supervisor Dr. Christopher Weisener for the opportunity to pursue this research and for all the feedback and guidance as a mentor. I would also like to thank my co-supervisor Dr. Daniel Heath for his support and assistance. Additional thanks as well to my committee members Dr. James Pope and Dr Christina Semeniuk. As well thanks to the team in New Zealand for additional help with field work and project conceptualization including Dr. James Pope, Dr. Paul Weber, and Will Olds. I would also like to thank Dave Trumm and family for their hospitality during my stay in New Zealand, as well as CRL staff for all their assistance. Also, thanks for additional support from lab members including Daniel VanMensel and Thomas Reid for assistance in the field and sample preparation. Additional thanks to staff at GLIER including Sharon Mackie at the SEM facility, J.C. Barrette for assistance with the ICPOES analyses, as well as Russel Hepburn in the genomics lab. And finally, a huge thank-you to all my family and friends in Newfoundland, and to those made in GLIER.



## TABLE OF CONTENTS

DECLARATION OF CO-AUTHORSHIP / PREVIOUS PUBLICATION .....	iii
ABSTRACT.....	v
DEDICATION .....	vi
ACKNOWLEDGEMENTS .....	vii
LIST OF TABLES .....	xi
LIST OF FIGURES .....	xii
LIST OF APPENDICES .....	xiv
LIST OF ABBREVIATIONS/SYMBOLS.....	xvi
Chapter 1 Introduction to acid mine drainage (AMD), remediation options, and associated risks.....	1
1.1 Environmental concern and scope of Acid Mine Drainage (AMD) .....	1
1.2 Chemistry and microbiology of AMD .....	2
1.3 Remediation options.....	4
1.4 Mussel shells as a bioreactor substrate.....	5
1.5 MSB limitations and risk due to sludge accumulation.....	7
1.6 Current options for storage of AMD remediation sludge .....	8
1.7 Research Goal .....	9
1.8 Hypotheses .....	9
1.8.1 Chapter Two hypothesis .....	9
1.8.2 Chapter Three Hypothesis.....	10
1.9 Research objectives .....	11

1.10	References .....	13
Chapter 2 Biogeochemical characterization of metal behavior from novel mussel shell bioreactor sludge residues .....		
2.1	Introduction .....	17
2.2	Materials and Methods .....	20
2.2.1	Site Description and Laboratory Incubations.....	20
2.2.2	Microsensors and Diffusive Flux Calculations .....	22
2.2.3	Geochemical Phase Description .....	23
2.2.4	Microbial Community Analyses .....	27
2.3	Results and Discussion.....	29
2.3.1	Oxygen and Hydrogen Sulfide Flux .....	29
2.3.2	Geochemical Phase Classification Using Two Methods to Quantify Microbial and Atmospheric Effects.....	32
2.3.3	Community Structure Shifts as a Function of Anoxic and Oxidic Incubation Environments.....	39
2.3.4	Biogeochemical Connections of AMD Sludge, and Associated Risks.....	46
2.4	Conclusions .....	52
2.5	References .....	54
Chapter 3 Summary of Mussel shell bioreactor sludge using field leaching columns as a comparison to laboratory mesocosms .....		
3.1	Introduction .....	59

3.2	Methods .....	61
3.2.1	Experimental Design.....	61
3.2.2	Micro sensors and diffusive flux calculations.....	63
3.2.3	Metal analysis from flow through.....	64
3.2.4	Geochemical phase descriptions .....	64
3.2.5	Hydrological predictions.....	65
3.3	Results and discussion.....	66
3.3.1	Chemical profiles and flux.....	66
3.3.2	Time series .....	70
3.3.3	Geochemical phase descriptions .....	75
3.3.4	Lifespan predictions based on mass balance of calcium.....	79
3.4	Conclusions .....	82
3.5	References .....	83
Chapter 4	Conclusions and Future Work .....	87
4.1	Conclusions and implications.....	87
4.2	Future work .....	89
4.3	References .....	92
APPENDIX	.....	93
VITA AUCTORIS	.....	110

## LIST OF TABLES

<b>Table 2.1</b> Selective geochemical extractions used. ....	26
<b>Table 2.2</b> Chemical and physical properties of sediment (diffusivity and flux) and water cap (pH) for all incubations for each month sampled.....	30
<b>Table 2.3</b> Alpha rarefaction showing average diversity metrics. ....	41
<b>Table 3.1</b> Metals (mg) released per kg of sludge in one month, calculated from a average over a 22 month period. ....	73
<b>Table 3.2</b> Chemical phase extractions for the final shaded cells identify which samples are significantly different based on a t-test. ....	78

## LIST OF FIGURES

<b>Figure 2.1</b> SEM analysis. ....	34
<b>Figure 2.2</b> PCA scatterplot for the Oxyhydroxide mineral phases in all four experimental conditions. ....	37
<b>Figure 2.3</b> PCoA of the top 1000 OTUs. ....	42
<b>Figure 2.4</b> Heatmap of the relative abundance of normalized counts for the top 15 most abundant classes. ....	45
<b>Figure 2.5</b> CCA plot using PCA components as environmental variables for each geochemical phase. ....	47
<b>Figure 2.6</b> Most abundant Genera in the final oxic and anoxic timepoints, as well as the initial in situ bacteria. ....	50
<b>Figure 3.1</b> Schematic of field experiment showing the saturated (left) and unsaturated (right) flow through columns and collection containers. ....	62
<b>Figure 3.2</b> Oxygen (black) and hydrogen sulfide (red) concentration profiles, in mg/l (oxygen) and $\mu\text{mol/L}$ (hydrogen sulfide). ....	68
<b>Figure 3.3</b> Leaching columns after one year, showing the saturated (top) and unsaturated (bottom). ....	69
<b>Figure 3.4</b> pH of the effluent water measured monthly on site, compared to the averagely monthly rainfall in mm near the mine site. ....	71
<b>Figure 3.5</b> Time series for sulfate, iron, and zinc in mg/l for both the saturated and unsaturated columns, compared to the average rainfall for the area. ....	74

**Figure 3.6** An updated figure from DiLoreto et al., (2016a) showing flow rates from 2012 to 2017. ....80

**Figure 3.7** Calcium concentrations of the inflow and outflow from the MSB, as well as the outflow-inflow which describes the amount of calcium dissolved from the mussel shells. ....81

## LIST OF APPENDICES

### Appendix Figures

<b>Figure A 1</b> PCA of the bioavailable showing PC1 and PC1 (top) and the metal loadings (bottom).....	93
<b>Figure A 2</b> Oxyhydroxide loadings for PC1 (top) and PC2 (bottom).....	94
<b>Figure A 3</b> PCA of the Strong acid extractable showing PC1 and PC1 (top) and the metal loadings (bottom). ....	95
<b>Figure A 4</b> PCA of the water soluble phase showing PC1 and PC1 (top) and the metal loadings (bottom). ....	96
<b>Figure A 5</b> PCA of the weakly bound to oxide phase showing PC1 and PC1 (top) and the metal loadings (bottom). ....	97
<b>Figure A 6</b> Rarefaction of each sample used in the analysis.....	104
<b>Figure A 7</b> Oxyhydroxide phase extraction for the field column experiments.....	105
<b>Figure A 8</b> Bioavailable (associated with organic matter).....	106
<b>Figure A 9</b> Water soluble phase extraction for the field column experiments.....	107
<b>Figure A 10</b> Strong acid extractable phase extraction for the field column experiments. Green (UN) represents the unsaturated, yellow (Initial) is the initial sludge, and Black (SAT) are samples from the saturated column.....	108
<b>Figure A 11</b> Metals weakly bound to iron oxides phase extraction for the field column experiments.. ....	109

## Appendix Tables

<b>Table A 1</b> PC scores for each geochemical phase used in the CCA .....	98
<b>Table A 2</b> Geochemical bioavailable phase data showing average (Ave) and standard deviation (SD) for each incubation environment and the initial mg/L. ....	99
<b>Table A 3</b> Geochemical oxyhydroxide phase data showing average (Ave) and standard deviation (SD) for each incubation environment and the initial in mg/L. ....	100
<b>Table A 4</b> Geochemical strong acid extractable phase data showing average (Ave) and standard deviation (SD) for each incubation environment and the initial in mg/L. ....	101
<b>Table A 5</b> Geochemical water-soluble extractable phase data showing average (Ave) and standard deviation (SD) for each incubation environment and the initial in mg/L. ....	102
<b>Table A 6</b> Geochemical phases associated with weakly bound oxides data showing average (Ave) and standard deviation (SD) for each incubation environment and the initial in mg/L. ....	103



## **LIST OF ABBREVIATIONS/SYMBOLS**

AMD- Acid Mine Drainage

ARD- Acid Rock Drainage

CCA- Canonical Correspondence Analysis

MSB- Mussel Shell Bioreactor

OTU- Operational Taxonomic Unit

PAF- Potentially Acid Forming

PCA- Principle Component Analysis

PC-Principle Component

PCoA- Principal Coordinates Analysis

SRB- Sulfate Reducing Bacteria

# **Chapter 1**

## **Introduction to acid mine drainage (AMD), remediation options, and associated risks**

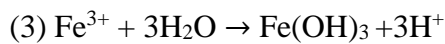
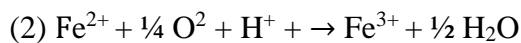
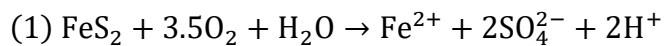
### **1.1 Environmental concern and scope of Acid Mine Drainage (AMD)**

Acid mine drainage (AMD) is an anthropogenic point source of pollution, that affects many mine impacted ecosystems around the world both aquatic and terrestrial (Bridge 2004). The contaminants (e.g. metals, acidity, DOC and turbidity) released by mining activities can have lasting effects on downstream aquatic environments if not properly managed (Armitage et al. 2007; Mayes et al. 2009). Many metal contaminated sites arise from “legacy” mining sites. In these cases, there is often little monitoring and funding for any remediation management. There are many orphan sites around the world, for example, in Canada there are over 10 000 legacy mines, while the United States accounts for over 600 000 (Worrall et al. 2009). Contamination from mining activity is usually a result of improper storage of uneconomical waste rock which is produced in high quantities during ore extraction from active mines. In just one year (2008) Canada produced 217 million tonnes of mine tailings and 256 tonnes of waste rock (Statistics Canada 2012). Mine tailings and waste rock can be produced by either open-pit or underground mining as both tend to bring sulfide minerals to the surface, causing previously stable metals to be oxidized and potentially released (Blowes et al. 2013). Open pit mining can also cause release of metals by leaving rock walls exposed, if they contain sulfide minerals. These mines can have extremely large surface areas (4km wide

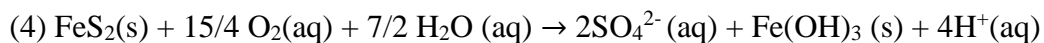
and 1.2 km deep for example), and will undergo oxidation for as long as they are exposed (Blowes et al. 2013).

## 1.2 Chemistry and microbiology of AMD

AMD is a by-product of the oxidation of sulfides such as pyrite ( $\text{FeS}_2$ ), a common mineral in both coal, base-metal (e.g. Ni, Cu), and gold mines. Pyrite oxidation is a process involving biological, chemical, and electrochemical reactions and has been widely reviewed (Evangelou and Zhang 1995; Akcil and Koldas 2006; Schippers et al. 2010a; Blowes et al. 2013; Amos et al. 2015; Nordstrom et al. 2015). Briefly, pyrite reacts with atmospheric oxygen and water to form sulfate, ferrous iron, and 2 moles of  $\text{H}^+$  for every mol of pyrite (equation 1) (Nordstrom 1985; Blowes et al. 2013). Ferrous iron can be further oxidized producing ferric iron (equation 3). Ferric iron ( $\text{Fe}^{3+}$ ) can also act as an oxidizer producing oxyhydroxides such as ferrihydrite and 4 moles of  $\text{H}^+$  further decreasing the pH.



These reactions are combined in an overall equation (4) that results in sulfate, iron precipitate, and high acidity.



Equations 1 through 4 demonstrate how Fe, sulfate, and acidic water can be generated by AMD. Metals from a mine site, however, are not limited to Fe and sulfate as the

surrounding geology of a mine will determine the specific metals which contaminate downstream environments. The waste rock or tailings can be comprised of minerals such as pyrite ( $\text{FeS}_2$ ), sphalerite ( $\text{ZnS}$ ), pyrrhotite ( $\text{Fe}_{1-x}\text{S}$ ), arsenopyrite ( $\text{FeAsS}$ ), galena ( $\text{PbS}$ ), chalcopyrite ( $\text{Cu}_5\text{FeS}_4$ ), and cinnabar ( $\text{HgS}$ ). In an AMD environment many of these minerals will be unstable and metals such as Zn, As, Pb, Hg, Fe, and Cu will leach out of the waste rock if uncontained.

The rate of dissolution of sulfide minerals can increase with the presence of bacteria (Singer and Stumm 1970), as the bacteria oxidize the hydrogen sulfide that is produced during acid dissolution of certain sulfide minerals producing sulfuric acid (Schippers et al. 1998). As AMD environments contain a variety of metals (e.g. Zn, Al, Cd) and pH's, the microbial community will be diverse, having specific gene expression pathways and adaptations which the microbes use to survive. Some examples revolve around maintaining a neutral cell pH despite the external extreme environment (Baker-Austin and Dopson 2007). Many of the microbes live under a range of chemolithoautotrophic, chemomixotrophic, or chemoheterotrophic conditions (Hallberg and Barrie Johnson 2001), and have the capability to oxidize iron sulfide minerals. Acidic environments also tend to have high concentrations of metals due to the increased solubility of minerals that may contain metals such as Zn, Cu, Mn, and As, depending on the local geology; therefore, organisms living in these environments must have some capability for metal resistance. Types of resistance mechanisms can include: permeability barriers (prevents metal from entering the cell), intra/extracellular binding (reduces toxic effect as the metal is immobile), enzymatic conversion (reduces metal to a less toxic form), and an alteration

of a cell component (reduces the toxicity of the metal to the cell) (Ji and Silver 1995; Huang et al. 2016).

### **1.3 Remediation options**

AMD runoff requires a remediation strategy that neutralizes acidity and immobilizes metals. Remediation of AMD can depend on abiotic or biotic reactions, either passive or active, and has been reviewed by Johnson and Hallberg (2005). Active abiotic remediation strategies are common in mining operations and involve the addition of an alkaline material such as lime or sodium hydroxide. This process increases the pH and produce hydroxides and carbonates in an iron rich “sludge.” This sludge is low density and fine grained, making it difficult to store and manage. This strategy of remediating AMD can be expensive and may only be appropriate for large-scale mining operations that are currently in operation.

For legacy AMD sites, the best option would be passive remediation as it tends to be more cost effective (DiLoreto et al. 2016a). Passive abiotic remediation can include limestone drains, which rely on the flow of water through an alkaline source. Armoring can occur in both oxygen-rich and oxygen-depleted environments, decreasing the longevity of this option especially in AMD waters with high aluminum and ferric iron (Hedin et al. 1994). Biotic passive remediation uses microorganisms to promote the mineralization of contaminate metals, and includes wetlands, compost reactors, and permeable reactive barriers (Gadd 2010; Zhang and Wang 2014; Nurjaliah Muhammad et al. 2016). Passive remediation often uses the biogeochemical cycling of metals by promoting the precipitation of sulfides in a reduced environment and can be completed in a system referred to as a bioreactor. These bioreactors often contain organic material to

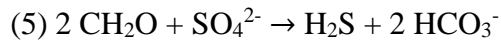
promote the growth of sulfur reducing bacteria (SRB), with the addition of alkaline material, such as limestone. SRB's are effective in remediating AMD as they help immobilize metals by promoting the formation of sulfides. The organic material in bioreactors vary and can include manure, wood chips, leaf litter, eggshells, or any other material easily available to the mine site (Benner et al. 2002; Zagury et al. 2002; Zhang and Wang 2016; Muliwa et al. 2018). Alkaline substrates used for remediation processes often include waste materials from other industries such as seafood, pulp and paper, wine, dairy, or other AMD treatment which may produce alkaline byproducts (Moodley et al. 2017). The source of alkalinity is important to sulfate reducing bioreactors as SRB tend to be most effective at  $\text{pH} < 7$  (Visser et al. 1996; Neculita et al. 2008; Tang et al. 2009; Serrano and Leiva 2017). The seafood industry produces waste in the form of calcium carbonate shells such as crab or mussels. These substrates often contain both calcium carbonate and organic material. Crab shells were found to promote reductive processes and produce short-chain organic compounds, which can facilitate the growth of SRB's but were found to be too expensive to obtain in high quantities (Robinson-lora and Brennan 2009).

#### **1.4 Mussel shells as a bioreactor substrate**

Small- and large-scale field systems in New Zealand have tested the potential of using mussel shell bioreactors (MSB), which are easily available and cheap for the mine sites to obtain (McCauley et al. 2009b; Uster et al. 2014; Trumm et al. 2015; DiLoreto et al. 2016a). Mussel shells have a high neutralizing capacity and contain enough organic matter in the form of chitin (5-12 wt%) and residual "meat" to promote the growth of SRB, which grow in anoxic conditions. Mussel shells were found to have higher metal

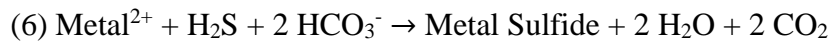
removal rates and alkalinity generation by 60-113% compared to traditional limestone (Uster et al. 2014).

These SRB use dissimilatory sulfate reduction pathways, such as



using organic material ( $\text{CH}_2\text{O}$ ) as an energy source and sulfate as the electron acceptor.

The  $\text{H}_2\text{S}$  produced can then react with metal ions present in the system to form monosulfides, in the reaction



with metals in the system such as Fe or Zn. The formation of metal sulfide precipitates essentially immobilizes the metal within the bioreactor. The source of organic carbon (e.g. acetate) in bioreactors is important as the rate of carbon degradation directly impacts the SRB, and therefore the longevity of the reactor (Logan et al. 2003).

Various configurations of MSB's have been studied including downflow and upflow reactors (McCauley et al. 2009a; Uster et al. 2014; Trumm et al. 2015). The upflow reactors are designed so that the AMD enters the bottom of the MSB where it is anoxic. This decreases the risk of iron oxide formation which impede performance by clogging reactors. Downflow reactors are currently being tested at both active and abandoned mine sites in New Zealand in 1000L plastic tubs. In one location, a series of three reactors was set up to study sequential metal precipitation. In addition to achieving a neutral pH, researchers found that 95-99% of Fe, Al, Ni, and Zn was removed in the first reactor and 0-22% of Mn was removed by the second and third (Trumm et al. 2015).

Though these reactors proved successful, they require a power generated pump in order for the water to flow from the bottom to the top and large-scale systems have not yet been tested for longevity.

Two downflow MSB's were studied at the Stockton coal mine in New Zealand, at the Manchester and Whirlwind seeps. The whirlwind reactor is full-scale, using approximately 362 tons of mussel shells in a trapezoidal design, in a pit with approximately 2m of mine water directed in by a retention pond upstream. This reactor is effective in increasing the pH and removing Fe, Al, NI, and Zn by 98% (DiLoreto et al. 2016b). During deconstruction of the MSB, DiLoreto et al (2016b) found distinct geochemical layers: allochthonous sediment (0-10mm), iron precipitate (11-40mm), aluminum (40-62mm), and reduced "unreacted shells" (62-1655mm) at the base of the reactor. Within these layers are distinct geochemistry and microbiology: the top was found to be oxic and acidic and have a high relative abundance of *proteobacteria*, and the bottom layers were reduced and circumneutral with increased *firmicutes* (DiLoreto et al. 2016a).

## **1.5 MSB limitations and risk due to sludge accumulation**

The top sediment layer of this reactor is the focus of this thesis, as previous studies have found it to be the limiting factor to the further use of downflow MSB. The sludge layer has low permeability, and the deposition of the sludge in the past 5 years (~15cm), has caused a decrease in the amount of AMD that the MSB is able to treat. Recently the bulk of the AMD which the MSB was designed to treat has been bypassing the reactor and is released into the downstream environment. The discharge rate of the reactor has decreased from around 5-6 L/s in 2014 to 1-2 L/s in 2016. This low discharge rate will



eventually result in early failure of the system. Though the MSB is a cost effective form of remediation, it relies on the reactor lasting up to 20 years to be comparable to other passive treatment options. For this reason, the sludge layer was removed in 2016 to promote an increased flow. Once the sludge was removed, it must be stored effectively to prevent further contamination, as the layer is acidic and contains potentially unstable metals such as Zn, and Al. Production of AMD remediation by-products are not uncommon and there are variety of methods used for storing these materials, as releasing them could have negative effects on the downstream environments (Zinck and Griffith 2005). Sediments can be released due to improper storage which can cause periodic deposition, or sudden, sometimes catastrophic events. Any of these events could cause long term toxic effects for organisms, either directly or indirectly. Heavy metals can bioaccumulate in the food web by entering root systems of plants directly (Kabata-Pendias, A.; Pendias 1992; Kumar et al. 1995), which are then consumed by larger animals.

## **1.6 Current options for storage of AMD remediation sludge**

AMD neutralization can produce from 20-135 000 tons of sludge per year from both passive and active technologies (Zinck and Griffith 2005). Zinck and Griffith reviewed 108 mine sites (66 within Canada) and found that 33 of those that store sludge, do so within a designated sludge pond, 12 were used as a tailings cover and 8 were stored using pit disposal. The remaining methods included mixing with tailings, used somehow within mine workings, stored in a heap leaching pad, sent to a landfill, or stored with waste rock. Demers et al. (2017) investigated the use of sludge as an oxygen barrier and found that in their case, the oxygen flux was too high and unstable to be useful. AMD sludge may also

be of economic interest (similar to tailings) if there is high weight percent of metals of value (Macías et al. 2017). Operating mines have found issues of sludge disposal, to be mainly space and unknown long-term stability issues.

## **1.7 Research Goal**

The goal of this thesis is to investigate risks associated with storage of AMD remediation sludge, specifically from the MSB located in New Zealand. This sludge may pose a unique problem as it is potentially acid forming (PAF) and formed within a novel bioreactor, which has only been tested once in a full-scale system. Potential storage options could include: a sludge pond, anoxic burial, sub-aerial storage along with tailings, or anoxic burial. As these storage options are a combination of anoxic and oxic conditions, a laboratory study was designed in order to investigate the risks associated with both storage environments and described in chapter 2. As the laboratory studies represent a controlled and consistent environment, a field study was designed to investigate how the sludge reacts under a dynamic environment, with seasonal effects such as rainfall. The field study will investigate two conditions; a saturated and an unsaturated environment. This study will be discussed in Chapter 3. Chapter 3 will also address the effect of the sludge on the predicted lifespan of the MSB, based on the dissolution of calcium carbonate.

## **1.8 Hypotheses**

### **1.8.1 Chapter Two hypothesis**

If we assume the accumulated sludge layer primarily contains a mix of iron and aluminium oxide mineral phases, there could be two potential options available for

storage; under oxic (deposition on the mine surface) or under anoxic conditions (deep burial or burial beneath the anoxic zone under a water cap, such as a tailings pond). Under oxic conditions, stability of compounds is expected to remain questionable since many metals associated with these oxides may be either physically or chemically sorbed species. It is predicted that there will be an increased risk factor of metal stability and a higher potential for chemical transport, which could possibly be due to the presence of oxidizing microorganisms. In contrast, under a situation of burial (e.g. anoxic or anaerobic condition) the oxides within the sludge may undergo active microbial dissolution, this would also pose a risk to metal transport unless a physical metal sequestration mechanism is present such as sulfide formation. If SRB are present, they would increase the formations of sulfides, but it is unknown if the sludge has an active community, as it is sourced from an oxic region of the reactor. Here I assume that the metals released due to oxides contained in the sludge material will be more stable under anoxic conditions, due to sulphide sequestration. These predictions will be addressed through a series of laboratory mesocosm discussed in supporting research objectives.

### **1.8.2 Chapter Three Hypothesis**

When the sludge is placed under a more dynamic condition, it is assumed that this will cause metals to leach out due to rainfall. In periods of increased rainfall, I predict that increased metals will be leached out, especially those contained in the water-soluble phases. Other labile phases which could undergo dissolution under rainfall include those metals weakly bound to iron oxides, and those associated with organic matter. Specific metals of interest within these phases include Zn, Mn, and Fe. The two conditions studied are unsaturated and saturated, which may have different leaching patterns. I predict that

the unsaturated sludge will have an increased dissolution of labile metals compared to the saturated. Other studies have found that when AMD remediation sludge was stored in unsaturated environments, it can cause preferential pathways for oxic waters to increase oxidation and dissolution deep into the sediment (Demers et al. 2017). For this reason, a saturated environment (i.e. with a water cap) will have increased stability of labile metals, compared to the unsaturated.

## **1.9 Research objectives**

The main research objective of this thesis is to identify potential risks associated with storage conditions of AMD remediation sludge. Chapter Two summarizes the laboratory study, which incubated the sludge under oxic and anoxic conditions to represent the two storage categories. The first objective of Chapter Two is to address the physicochemical changes under oxic and anoxic storage with and without an active microbial community. To achieve this, a chemical control for the mesocosm was sterilized, and diffusive flux was calculated for each environment. This will determine how both  $O_2$  and  $H_2S$  move across the sediment water interface, and the role of microbial activity. The second objective is to determine the changes of geochemistry within each condition and investigate the role of possible chemolithotrophic activity from bacterial communities by comparing the sterilized and active mesocosms. The third objective of Chapter Two was to identify changes in the microbial community by completing a taxonomic survey of the environmental extremes. This will help identify any known SRB or oxidizing bacteria were in either of the environments. The taxonomy of the microbial communality was correlated with the geochemistry to identify apparent microbial impacts on the sludge.

Chapter Three uses a field study which assessed the metal release in the natural environment, where it could interact with rainwater on the mine site. The first objective of chapter three was to compare leaching experiments which were designed to mimic a saturated and an unsaturated environment. A saturated storage environment represented storage under a water cap in the transition zone from oxic to anoxic. The unsaturated represented storage on the surface of the mine and fluctuated between dry and wet patterns due to rainfall. In order for comparisons to the laboratory study, physicochemical changes and geochemical phases were also addressed in this chapter, as well as concentrations of the metals from the flow through systems. The second objective of this chapter is to calculate the longevity of the original MSB, with and without the effects of the sludge layer. This will help influence decisions on further uses of the MSB and management practices.

Finally, Chapter Four will summarize the conclusions from the previous chapters and make recommendations for future studies.

## 1.10 References

- Akcil A, Koldas S (2006) Acid Mine Drainage (AMD): causes, treatment and case studies. *J Clean Prod* 14:1139–1145. doi: 10.1016/j.jclepro.2004.09.006
- Amos RT, Blowes DW, Bailey BL, et al (2015) Waste-rock hydrogeology and geochemistry. *Appl Geochemistry* 57:140–156. doi: 10.1016/j.apgeochem.2014.06.020
- Armitage PD, Bowes MJ, Vincent HM (2007) Long-term changes in macroinvertebrate communities of a heavy metal polluted stream: the river Nent (Cumbria, UK) after 28 years. *River Res Appl* 23:997–1015. doi: 10.1002/rra.1022
- Baker-Austin C, Dopson M (2007) Life in acid: pH homeostasis in acidophiles. *Trends Microbiol* 15:165–171. doi: 10.1016/J.TIM.2007.02.005
- Benner SG, Blowes DW, Ptacek CJ, Mayer KU (2002) Rates of sulfate reduction and metal sulfide precipitation in a permeable reactive barrier. 17:301–320.
- Blowes DW, Ptacek CJ, Jambor JL, et al (2013) *The Geochemistry of Acid Mine Drainage*, 11th edn. Elsevier Ltd.
- Bridge G (2004) CONTESTED TERRAIN: Mining and the Environment. *Annu Rev Environ Resour* 29:205–259. doi: 10.1146/annurev.energy.28.011503.163434
- Demers I, Mbonimpa M, Benzaazoua M, et al (2017) Use of acid mine drainage treatment sludge by combination with a natural soil as an oxygen barrier cover for mine waste reclamation: Laboratory column tests and intermediate scale field tests. *Miner Eng* 107:43–52. doi: 10.1016/j.mineng.2016.11.017
- DiLoreto ZA, Weber PA, Olds W, et al (2016a) Novel cost effective full scale mussel shell bioreactors for metal removal and acid neutralization. *J Environ Manage.* doi: 10.1016/j.jenvman.2016.09.023
- DiLoreto ZA, Weber PA, Weisener CG (2016b) Solid phase characterization and metal deportment in a mussel shell bioreactor for the treatment of AMD, Stockton Coal Mine, New Zealand. *Appl Geochemistry* 67:133–143. doi: 10.1016/j.apgeochem.2016.02.011
- Evangelou VP (Bill), Zhang YL (1995) A review: Pyrite oxidation mechanisms and acid mine drainage prevention. *Crit Rev Environ Sci Technol* 25:141–199. doi: 10.1080/10643389509388477
- Gadd GM (2010) Metals, minerals and microbes: Geomicrobiology and bioremediation. *Microbiology* 156:609–643. doi: 10.1099/mic.0.037143-0
- Hallberg KB, Barrie Johnson D (2001) Biodiversity of acidophilic prokaryotes. *Adv Appl Microbiol* 49:37–84. doi: 10.1016/S0065-2164(01)49009-5

- Hedin RS, Watzlaf GR, Nairn RW (1994) Passive Treatment of Acid Mine Drainage with Limestone. *J Environ Qual* 23:1338. doi: 10.2134/jeq1994.00472425002300060030x
- Huang L-N, Kuang J-L, Shu W-S (2016) Special Series: Microbial Communities Microbial Ecology and Evolution in the Acid Mine Drainage Model System. doi: 10.1016/j.tim.2016.03.004
- Ji G, Silver S (1995) Bacterial resistance mechanisms for heavy metals of environmental concern. *J Ind Microbiol* 14:61–75. doi: 10.1007/BF01569887
- Johnson DB, Hallberg KB (2005) Acid mine drainage remediation options: A review. *Sci Total Environ* 338:3–14. doi: 10.1016/j.scitotenv.2004.09.002
- Kabata-Pendias, A.; Pendias H (1992) Trace Elements In.
- Kumar PBAN, Dushenkov V, Motto H, Easkin I (1995) Phytoextraction: The Use of Plants to Remove Heavy Metals from Soil. *Plant Met Interact Emerg Remediat Tech* 29:361–384. doi: 10.1016/B978-0-12-803158-2.00015-1
- Logan M, Ahmann D, Figueroa L (2003) Assessment of Microbial Activity in Anaerobic Columns Treating Synthetic Mine Drainage 1. *Jt Conf 9th Billings L Reclam Symp 20th Annu Meet Am Soc Min Reclam June 3-6, 2003* 0658. doi: 10.21000/JASMR03010658
- Macías F, Pérez-López R, Caraballo MA, et al (2017) Management strategies and valorization for waste sludge from active treatment of extremely metal-polluted acid mine drainage: A contribution for sustainable mining. *J Clean Prod* 141:1057–1066. doi: 10.1016/J.JCLEPRO.2016.09.181
- Mayes WM, Johnston D, Potter HAB, Jarvis AP (2009) A national strategy for identification, prioritisation and management of pollution from abandoned non-coal mine sites in England and Wales. I.: Methodology development and initial results. *Sci Total Environ* 407:5435–5447. doi: 10.1016/J.SCITOTENV.2009.06.019
- McCauley CA, O’Sullivan AD, Milke MW, et al (2009) Sulfate and metal removal in bioreactors treating acid mine drainage dominated with iron and aluminum. *Water Res* 43:961–970. doi: 10.1016/j.watres.2008.11.029
- Moodley I, Sheridan CM, Kappelmeyer U, Akcil A (2017) Environmentally sustainable acid mine drainage remediation: Research developments with a focus on waste/by-products. *Miner Eng*. doi: 10.1016/J.MINENG.2017.08.008
- Muliwa AM, Leswif TY, Onyango MS (2018) Performance evaluation of eggshell waste material for remediation of acid mine drainage from coal dump leachate. *Miner Eng* 122:241–250. doi: 10.1016/J.MINENG.2018.04.009
- Neculita CM, Zagury GJ, Bussière B (2008) Effectiveness of sulfate-reducing passive bioreactors for treating highly contaminated acid mine drainage: II. Metal removal

- mechanisms and potential mobility. *Appl Geochemistry* 23:3545–3560. doi: 10.1016/j.apgeochem.2008.08.014
- Nordstrom DK (1985) The rate of ferrous iron oxidation in a stream receiving acid mine effluent. *Sel Pap Hydrol Sci* 113–119.
- Nordstrom DK, Blowes DW, Ptacek CJ (2015) Hydrogeochemistry and microbiology of mine drainage: An update. *Appl Geochemistry*. doi: 10.1016/j.apgeochem.2015.02.008
- Nurjaliah Muhammad S, Mohd Kusin F, Syakirin Md Zahar M, et al (2016) Environmental Technology Passive bioremediation technology incorporating lignocellulosic spent mushroom compost and limestone for metal-and sulfate-rich acid mine drainage. doi: 10.1080/09593330.2016.1244568
- Robinson-lora MA, Brennan RA (2009) Bioresource Technology Efficient metal removal and neutralization of acid mine drainage by crab-shell chitin under batch and continuous-flow conditions. *Bioresour Technol* 100:5063–5071. doi: 10.1016/j.biortech.2008.11.063
- Schippers A, Breuker A, Blazejak A, et al (2010) The biogeochemistry and microbiology of sulfidic mine waste and bioleaching dumps and heaps, and novel Fe(II)-oxidizing bacteria. *Hydrometallurgy* 104:342–350. doi: 10.1016/J.HYDROMET.2010.01.012
- Schippers A, Jozsa P-G, Sand W (1998) Evaluation of the efficiency of measures for sulphidic mine waste mitigation. *Appl Microbiol Biotechnol* 49:698–701. doi: 10.1007/s002530051234
- Serrano J, Leiva E (2017) Removal of arsenic using acid/metal-tolerant sulfate reducing bacteria: A new approach for bioremediation of high-arsenic acid mine waters. *Water (Switzerland)* 9:1–12. doi: 10.3390/w9120994
- Singer PC, Stumm W (1970) Acidic Mine Drainage: The Rate-Determining Step. *Source Sci New Ser* 167:1121–1123.
- Statistics Canada (2012) Human Activity and the Environment: Waste management in Canada.
- Tang K, Baskaran V, Nemati M (2009) Bacteria of the sulphur cycle: An overview of microbiology, biokinetics and their role in petroleum and mining industries. *Biochem Eng J* 44:73–94. doi: 10.1016/j.bej.2008.12.011
- Trumm D, Ball J, Pope J, Weisener C (2015) Passive Treatment of ARD Using Mussel Shells – Part III : Technology Improvement and Future Direction. 10th Int Conference Acid Rock Drain IMWA Conf 1–9.
- Uster B, O’Sullivan AD, Ko SY, et al (2014) The Use of Mussel Shells in Upward-Flow Sulfate-Reducing Bioreactors Treating Acid Mine Drainage. *Mine Water Environ* 34:442–454. doi: 10.1007/s10230-014-0289-1



- Visser A, Hulshoff Pol LW, Lettinga G (1996) Competition of methanogenic and sulfidogenic bacteria. *Water Sci Technol* 33:99–110. doi: 10.1016/0273-1223(96)00324-1
- Worrall R, Neil D, Brereton D, Mulligan D (2009) Towards a sustainability criteria and indicators framework for legacy mine land. *J Clean Prod* 17:1426–1434. doi: 10.1016/J.JCLEPRO.2009.04.013
- Zagury J, Cl B, Cocos IA (2002) Multiple factor design for reactive mixture selection for use in reactive walls in mine drainage treatment. 32:167–177.
- Zhang M, Wang H (2014) Organic wastes as carbon sources to promote sulfate reducing bacterial activity for biological remediation of acid mine drainage. *Miner Eng* 69:81–90. doi: 10.1016/j.mineng.2014.07.010
- Zhang M, Wang H (2016) Preparation of immobilized sulfate reducing bacteria (SRB) granules for effective bioremediation of acid mine drainage and bacterial community analysis. doi: 10.1016/j.mineng.2016.02.008
- Zinck J, Griffith W (2005) CANMET Mining and Mineral Sciences Laboratories. *Mine Environ Neutral Drain* 1–60.

## **Chapter 2**

### **Biogeochemical characterization of metal behavior from novel mussel shell bioreactor sludge residues**

#### **2.1 Introduction**

Acid rock drainage (ARD) is a naturally occurring process that is amplified by mining activities and becomes an anthropogenic point source of pollution referred to as acid mine drainage (AMD) that commonly has a pH of <4. The geochemistry of waste rock will determine the specific contaminants in AMD, but can include high concentrations of Fe, Sulfate, Cu, Zn, Mn, Mg, Hg, As, Pb, and other metals. AMD affects many ecosystems around the world, both aquatic and terrestrial (Bridge 2004; Akcil and Koldas 2006) and occurs when waste rock containing sulfides are oxidized, producing ferric iron ( $\text{Fe}^{3+}$ ) which can act as an oxidizer in the absence of oxygen (Nordstrom 1985). Surrounding streams can be contaminated by AMD and precipitates (such as schwertmannite and ferrihydrite) and, if not properly managed (Armitage et al. 2007; Mayes et al. 2009), will have toxic effects on benthic organisms (Han et al. 2017). Rates of AMD reactions can increase in the presence of bacteria (Singer and Stumm 1970) as microbes oxidize hydrogen sulfide produced during the dissolution of sulfide minerals producing sulfuric acid (Schippers et al. 1998).

Remediation of AMD is traditionally divided into two categories: passive and active systems. Active systems involve the continued addition of alkaline substances to increase the pH and have higher capital and operational costs relative to passive treatments. Passive remediation refers to the use of wetland systems, both natural and manmade, and

usually requires little maintenance and comparatively lower costs, making it the preferred choice for legacy sites or sites at closure. A novel full-scale mussel shell bioreactor (MSB) was constructed in 2011 and is currently treating an AMD seep at a coal mine on the west coast of the South Island of New Zealand. The MSB removes approximately 99% of all metals and raises the pH from 3.3 to 7.9 and is estimated to be 15 times more cost-effective than other methods (DiLoreto et al. 2016a). The MSB has distinct geochemical layers including: an allochthonous sediment/sludge layer (0–15 cm), Fe oxide reacted shell layer (15–35 cm), Al oxide reacted shell layer (35–60) and reduced unreacted shells (60–130 cm). The efficiency of the reactor has decreased with time due to the build-up of fine-grained sediment and AMD remediation byproducts, referred to as sludge. This reflects a common problem in AMD remediation strategies: dissolved mine contaminant effluents are treated, but sludge is produced in large quantities, creating the need for a multi-step maintenance plan.

Traditional methods of AMD neutralization can produce up to 135,000 tons of AMD sludge per year from both passive and active technologies (Zinck and Griffith 2005). Few studies have examined the weathering and leaching behavior of these by-products, and there are even fewer on the effects of microbial activity on these materials. A review of sludge management practices found that the most common storage practice was within a sludge pond (Zinck and Griffith 2005). Other methods of management included mixing sludge with other tailings or waste rock dumps, pit disposal, or reusing it within the mine (such as using it for neutralization strategies). Some other recent applications of AMD sludge include mixing it with natural soils as an oxygen barrier for the storage of mine tailings to reduce further production of AMD (Demers et al. 2017). Other studies

explored the possibility of recovering elements of economic interests as well as classifying the risk associated with sludge storage (Macías et al. 2017). Some concerns regarding sludge storage by mines listed in a review by Zinck and Griffith (2005) were: space for disposal, the long-term stability of the sludge, and that sludge management requires a site-specific approach. The sludge in this study presents a unique problem as the downflow MSB is based on novel technology still being tested. In addition, this sludge is potentially acid-forming, while other AMD sludges may be alkaline.

The sludge layer has accumulated over a four-year period and has significantly impacted the performance of the existing MSB. The sediment sludge layer was found to contain gibbsite (an aluminum hydroxide), ferrierite, and have a pH of 3 (DiLoreto et al. 2016b). The top sludge layer was removed in 2016 to increase the permeability and lifespan of the MSB. As part of their reclamation strategy, the mine site is currently interested in the behavior and functionality of the sludge. This study is focused on the upper sludge layer and presents the geochemical stability in two potential storage environments, oxic and anoxic with and without the influence of microbes. The purpose of this study is to determine if this sludge may be able to be used for further mining management, such as repurposing with soil blends, and if not, how the sludge will behave if stored in an anoxic environment. The anoxic incubation also provided a way to test if the microbial community from the oxic portion of the bioreactor could thrive in an anoxic environment and if they would increase the stability of the sludge. In this study, we investigate the physicochemical and biological influence of an AMD sludge layer under conditions of anoxia and oxygen saturation. A series of laboratory mesocosms were designed to simulate aerobic and anoxic storage/disposal options and to characterize the

chemical and biological stability. Here we determine oxygen and hydrogen sulfide diffusive flux, metal stability, and microbial community drivers which can impact the sludge stability in the presence/absence of oxygen as a function of aging.

## **2.2 Materials and Methods**

### **2.2.1 Site Description and Laboratory Incubations**

Details of the MSB and mine site have been described in past studies (McCauley et al. 2010; Trumm et al. 2015; DiLoreto et al. 2016a; DiLoreto et al. 2016b). The coal mine is located on the west coast of New Zealand within the Brunner Coal Measures, a formation containing 1–5 wt% pyrite and is potentially acid forming (PAF) (Pope et al. 2010; Weisener and Weber 2010; Trumm et al. 2015). This resulted in AMD runoff high in Fe and Al as well as trace metals including As, Cd, Ni, Pb, Tl, and Zn (McCauley et al. 2009a; McCauley et al. 2009b; McCauley et al. 2010). Numerous on-site management practices are currently in place, including: active treatment using CaO to neutralize AMD, barrier systems to exclude oxygen and water, and strategic mine planning, which is summarized in DiLoreto et al., (2016b). The MSB was built with 362 tons of mussel shells which have a range of 88–95 wt% CaCO<sub>3</sub> with the remaining weight made up of organic material and has been treating an AMD seep since late 2012. Since then it has undergone two sampling periods over two years where it was characterized both microbially and geochemically (DiLoreto et al. 2016a; DiLoreto et al. 2016b).

Bulk sediment samples were collected from the first 10 cm (sediment/sludge layer) of the MSB in February 2016, as well as mine water, which was obtained from the inlet of the MSB. The samples were stored and shipped under refrigeration to minimize

geochemical alterations until experimental set up. A  $2 \times 2$  experimental design (with replicates) allowed two environmental conditions (anoxic and oxic) to be tested, and determined the microbial impact (biotic vs. abiotic) on the sludge. This study design has been used in numerous past studies to address environmental impacts of various materials (Chen et al. 2013; Boudens et al. 2016; Reid et al. 2016). The four experimental conditions discussed in this study are biotic anoxic, abiotic anoxic, biotic oxic, and abiotic oxic. Differences between the abiotic and biotic mesocosms are referred to as microbial effects, while variations between the anoxic and oxic mesocosms are referred to as atmospheric effects. Sediment and water for the abiotic mesocosms were sterilized by gamma irradiation at the McMaster Institute of Applied Radiation Services (McIARS) in Hamilton, Ontario, Canada. An anaerobic chamber achieved anoxic environmental conditions, filled with approximately 95%  $N_2$  and 5%  $H_2$ , and with moisture control. The oxic mesocosms were left in the natural laboratory atmosphere, just outside the chamber. All mesocosms were duplicated and covered by black fabric to allow minimal light interference. These mesocosms mimicked conditions of deep burial and/or anoxic ponds as well as storage on the mine surface (oxic). Approximately 2 kg of sediment and 1 L of cap water (AMD water from inflow of the MSB) was placed in sterilized 4 L Camwear<sup>®</sup> containers with lids (but not airtight) from the Cambro Manufacturing Company. Sediment samples were taken after approximately 4, 12, and 20 weeks for microbial analysis from the surface of the sludge within the mesocosm (first 1 cm). A spatula was used to collect samples from different sections during each sampling period, as to not sample an area which was previously disturbed. Final samples (approximately 15 g) from the top 1 cm of the sediment, near the center of the mesocosm, were collected for

geochemical analysis. This included solid phase analysis using a scanning electron microscope and selective geochemical extractions.

### 2.2.2 Microsensors and Diffusive Flux Calculations

HS<sup>-</sup>, O<sub>2</sub>, and redox microelectrode sensors (Unisense Science, Denmark) were used to measure vertical gradients approximately 1 cm above and 1 cm below the sediment water interface, a method developed by Revsbech, (1989) but more explicitly following methods by Reid et al. (2016). The sensor measurements were taken near the center of the mesocosm, and before each sediment sampling period, so the profiles would be undisturbed. Sensor manipulation was done via a computer fitted with SensorTrace Pro software and the Unisense Microsensor Multimeter model PA2000. The microsensors have 10(H<sub>2</sub>S)-500 (oxygen) µm glass tips and take precise and continuous measurements using an automated micro manipulator, able to take measurements every 100 µm. Calibration and pre-polarization guidelines followed the Unisense prescribed procedures (2017). Profiles were taken at 4 and 20 months during the incubation for every mesocosm.

A diffusivity sensor (50 µm) was used to measure diffusivity constants in all mesocosms at the end of the incubation period. This required using a two-point calibration (Revsbech et al. 1998) and an inert gas, in this case, 5% H<sub>2</sub> mixed with 95% N<sub>2</sub>. A slope derived from the profiles of O<sub>2</sub> and H<sub>2</sub>S<sup>-</sup> is used along with the diffusivity measurement in the following equation:

$$J(x) = -\phi D(x) \frac{dc(x)}{dx} [\text{cm}^2\text{S}^{-1}] \quad (1)$$

$J(x)$  is flux;  $-\partial D(x)$  is the diffusivity measured using the diffusivity sensor on the sediment; and  $dC(x)/dx$  is the slope of the  $\text{HS}^-$  and  $\text{O}_2$  concentration profile measured along the sediment-water interface.

### 2.2.3 Geochemical Phase Description

#### *Scanning Electron Microscopy (SEM) and Particle Count Analysis*

Solid samples collected from the initial bioreactor sediment (time zero) and final timepoints were preserved (approximately 5 g) and made into polished thin-sections for mineral characterization by Scanning Electron Microscopy (SEM). The analysis was completed to determine geochemical differences in the sediment after incubation in oxic and anoxic conditions, and to determine any microbial effects (differences between biotic and abiotic). Analyses were performed using a FEI Quanta 200F, Environmental Scanning Electron Microscope (FEI, Eindhoven, The Netherlands) at high vacuum (20 kv) with a theoretical spot size of 2.6 nm, at the Great Lakes Institute for Environmental Research (GLIER), University of Windsor, (Windsor, ON, Canada). Visual inspections of mineral grains were completed using both backscattered electron (BSE) and secondary electron detectors (SE). The SEM was configured with an EDAX<sup>®</sup> SiLi detector (EDAX, Mahwah, NJ, USA) to analyze differences in the elemental composition of mineral grains in each mesocosm. EDAX Genesis Particle cluster analysis software (version 5.21) was used for particle counts and elemental composition. Duplicate areas were analyzed on each thin section at 1000 $\times$  magnification to account for particles sizes down to 1  $\mu\text{m}$ . Particles were identified by the software and counted based on their brightness under constant levels of contrast for every sample. This allowed for only particles of heavy elemental weight to be counted for the following elemental proportions: C, O, Mg, Al, Si,



S, K, Ca, Ti, Mn, Fe, Co, Cu, and Zn. Data for Figure 2.1 was normalized to 100% for Fe, S, and O to determine the presence of iron sulfides and iron oxides; however, all concentrations discussed in the text are normalized values for all elements selected on the EDAX detector.

### ***Selective Solid Phase Extractions***

In total, five geochemical extractions were completed on the final incubation samples to be compared with the initial sediment. Sediment was collected from the top 1 cm of the sludge using sterilized spatulas and put into sterilized 50 mL polypropylene centrifuge tubes (in triplicates). Samples were also taken from the top of the MSB to act as a time zero. All extractions were done using a 1:10 ratio of sediment to extractant fluid, specifically 3 g to 30 mL. The five extraction targets were as follows: water-soluble; bio-available (EDTA); amorphous oxyhydroxide phases (reducible); strong acid extractable; and metals weakly bonded to oxide phases (weak acid) following the same protocols as DiLoreto (2017) and described in Table 2.1. The sediment and extractant fluid within the tubes were shaken (using an orbital shaker) for 24 h, except for the strong acid extraction which was shaken for 21 days to achieve total extractable. The extractant fluid was filtered, acidified (for preservation), and then analyzed using a 700 series Agilent 720-ES ICP-OES system for heavy metals. Principle component analyses (PCA) were used to evaluate the chemical extraction data to determine the variation between experimental factors and the elements with the most substantial impact on each representative environment. Initial samples from the MSB were also included in the PCA and will serve as a time point zero, referred to as “initial”. PCA analysis also determined microbial effects based on clustering and PC scores; if the abiotic incubation clustered separately

from the biotic, then it was considered to have microbial effects. Using PAST, two-way ANOVA tests were also used to determine atmospheric or microbial effects on specific metals in each geochemical phase. Student t-tests were performed within Excel on individual samples to determine if significant differences existed between geochemical phases in the abiotic vs. microbially active incubations.

**Table 2.1** Selective geochemical extractions used.

<b>Target</b>	<b>Extractant</b>	<b>Citation</b>
Water-soluble	N purged milli Q water	Ribeta et al., (1995)
Bio-available	0.005 EDTA adjusted to pH 6	Fangueio at al. (2001)
Metals weakly bonded to oxide phases	0.5 M HCl	Heron et al., (1994)
Amorphous oxyhydroxide (reducible)	0.12 M sodium ascorbate; 0.17 M sodium citrate; 0.6 M NaHCO <sub>3</sub> , adjusted to pH 8	Amirbahman, (1998)
Strong acid extractable	5 M HCl	Heron at al., (1994)

## **2.2.4 Microbial Community Analyses**

### ***DNA Extraction and Sequencing Preparations***

Sediment samples (approximately 1 g) were collected for three-time points throughout the five-month incubation in triplicate from the first 1 cm of sediment from the laboratory incubation and stored at -80 °C. The initial samples collected from the field were flash frozen, stored in liquid nitrogen, and transported to a -80 °C freezer. DNA extractions, using 0.25 g of sample, were performed using MoBIO power soil DNA kits (Mobio Laboratories, Carlsbad, California) according to manufacturer protocols. Two-step PCRs were completed to amplify and barcode the DNA, according to the protocols laid out in Falk et al. (2018). However, in the current study, the V4-V5 regions of the 16S rRNA gene were amplified with the initial PCR using primers 515F-Y and 926R (Parada et al. 2016). Amplified DNA products were then individually barcoded by the sample (PCR 2), pooled according to band intensity by gel electrophoresis, and analyzed on the Agilent 2100 Bioanalyzer (Agilent Technologies, Santa Clara, United States) for quality and quantity determination. The pooled sample library was then sequenced on the Ion Torrent Personal Genome Machine (Life Technologies, Carlsbad, United States) at GLIER, University of Windsor, Canada.

### ***Community Structure Analysis***

Microbial taxonomic identification was completed using the MacQIIME 1.9.1 (Quantitative Insights into Microbial Taxonomy) pipeline (<http://qiime.org/>). The raw sequence file was demultiplexed, barcodes/adapters were removed, and sequences filtered for quality assurance. Sequences were cut off at a Phred score of 25, samples were removed with sequence counts less than 3000, and chimera sequences were identified and

removed using usearch61 (Edgar et al. 2011). Clustering of sequences into operational taxonomic units (OTUs) was performed by open-reference OTU using a 97% similarity threshold with the uclust algorithm (Edgar 2010). Taxonomy was also assigned by uclust, with a 90% consensus threshold, using the default GreenGenes database and normalized using DESeq2 (Love et al. 2014), as this method is acceptable for low replicate studies (<20) (Weiss et al. 2017).

Diversity indices were computed using the Shannon-Wiener (Lloyd and Ghelardi 1964) and Chao indices (Chao 1984) using the alpha diversity scripts by MacQiime. This determined if oxic or anoxic incubation environment altered diversity. Rarefaction curves were also produced using scripts within MacQiime, with sequences greater than 3000. Principal coordinates analysis (PCoA) was conducted using the R package for Amplicon-Sequencing-Based Microbial-Ecology (RAM) v1.2.1.3 on the top 1000 OTUs representing 80% of the total sequence reads for all samples. PCoA was used to determine if major differences existed between oxic, anoxic (all time points), and initial communities based on clustering. Further, microbial community differences between the oxic and anoxic mesocosm differential abundance analysis were assessed at an OTU level. Differential abundance of OTUs was computed using the DESeq2 method (Love et al. 2014).

In order to predict the broad functional changes in microbial diversity in oxic and anoxic environments, differences at the phylum level were examined. To determine major changes that are not detected at the phylum level, the top 15 classes that incorporate 80% of the sequences were analyzed. Differential abundance (described above) was also used to validate broad differences observed by relative abundance alone.

To compare the influence of environmental and chemical factors on the microbial diversity in oxic and anoxic environments, Canonical Correspondence Analysis (CCA) was used. Instead of using the individual metals for each geochemical phase, PC loadings from the PCA described in Section 2.3.2 were used as the environmental factors. The top 1000 OTUs, representing 80% of the total sequences, were used as the microbial response for the CCA plot.

## **2.3 Results and Discussion**

### **2.3.1 Oxygen and Hydrogen Sulfide Flux**

The diffusive flux of both oxygen and H<sub>2</sub>S were determined for the oxic and anoxic sludge incubations treatments respectively. Oxygen and hydrogen sulfide concentrations were measured in each mesocosm across the sediment-water interface to determine the concentration gradient. The abiotic incubations showed DO at 5.5–7.5 mg/L, which decreased to zero within 1 cm past the sediment-water interface (Table 2.2). In comparison, the biotic incubations showed less oxygen in the cap water with ~2–3 mg/L rapidly decreasing to 0 mg/L ~0.5 cm into the sediment. Oxygen concentrations are higher in the abiotic system as microbes produce reducing agents and consume oxygen. These oxygen profiles and apparent diffusivity (porosity\*diffusivity coefficient) were used to calculate flux. The redox potential across the sediment interface was also measured. ORP values remained consistent ranging from 262 (eV) to 229 (eV) in the oxic treatment over five months. In contrast, the anoxic treatments showed the development of reducing conditions (Table 2.2).

**Table 2.2** Chemical and physical properties of sediment (diffusivity and flux) and water cap (pH) for all incubations for each month sampled. Each number represents an average for each experimental condition. ND (not detected) was recorded for certain samples as oxygen was not present in the Anoxic, and H<sub>2</sub>S was not found in the abiotic mesocosms or the oxic.

Chemical Component	Month	Oxic		Anoxic	
		Biotic	Abiotic	Biotic	Abiotic
oxygen flux <sup>1</sup>	1	1.83	2.79	ND	ND
	5	1.21	6.23	ND	ND
H <sub>2</sub> S flux <sup>1</sup>	1	ND	ND	210	ND
	5	ND	ND	60.9	ND
O <sub>2</sub> (mg/L)	1	2.6	5.5	0	0
	5	3.01	7.1	0	0
HS (μmo/L)	1	0	0	8.7	5.96
	5	0	0	15	ND
Redox Potential	1	262	230	10	80
	5	229	300	-80	-100
pH	1	3.27	4.1	5.89	5.92
	5	3.24	3.74	5.19	4.87

<sup>1</sup> units: mmol m<sup>-2</sup> day<sup>-1</sup>.

In comparison to the abiotic, the calculated oxygen flux within the biotic incubations did not have a large shift from the first month to the final (from 1.21 to 1.83 mmol m<sup>-2</sup> day<sup>-1</sup>). Oxygen flux in the abiotic mesocosm increased from 2.79 mmol m<sup>-2</sup> day<sup>-1</sup> to 6.23 mmol m<sup>-2</sup> day<sup>-1</sup> based on the first and final month. These flux values were low compared to natural systems which have been reported up to 89 mmol m<sup>-2</sup> day<sup>-1</sup> in productive lakes (Thorbergssdóttir et al. 2004). In the biological system, oxygen was consumed during the formation of minerals observed at the interface very early on in the mesocosm experiment (within one month). The system reached a steady state quickly and therefore the biological and chemical demand for oxygen was low, though oxygen was still being consumed. The diffusivity constant was approximately 75% lower in the biotic mesocosm which may have been caused by the increase of iron oxides (possibly amorphous) which altered the porosity and the sediments ability to diffuse oxygen. This was supported by visual observations during the first month of the mesocosm, in which a bright orange precipitate formed on the surface of the sludge in the biotic trials. In the abiotic system, the higher diffusion coefficient allowed for significant diffusion of oxygen into the sediment compartment, uninhibited by biological consumption of oxygen. In this case, the biotic oxygen flux had a much steeper slope over a shorter depth. The difference in oxygen concentration in the overlying water was higher for the abiotic system, and resulted in a shallower depth concentration gradient. Observations of the abiotic system showed a change in sediment color at around four months, suggesting that at this time the sediment had oxidized at a slower rate than what was observed in the biotic system.

Under conditions of anoxia, a primary concern regarding sulfide-rich sludge is the evolution of hydrogen sulfide. To determine the potential flux of hydrogen sulfide from



the MSB sludge, several measurements were collected using the biotic and abiotic incubated materials. The abiotic incubations showed no significant H<sub>2</sub>S and therefore no flux was calculated. In contrast, the anoxic biotic incubations showed an elevated concentration of 8.7 µmol/L hydrogen sulfide at 1 cm below the sludge/water interface. The calculated hydrogen sulfide flux for both the first and final time points showed a decrease in H<sub>2</sub>S concentration from 210 to 60 mmol m<sup>-2</sup> day<sup>-1</sup>. Although no increase in H<sub>2</sub>S was observed in the water cap of these experiments, it suggests that the observed decrease of measurable sulfide flux may in part be due to secondary processes (e.g., sulfide precipitation or a decrease in sulfur reducing bacteria). This result is similar to those found in Reid et al. (2016) and was suggested to be related to the formation of sulfides causing an increase in porosity. Sulfides, such as FeS<sub>2</sub> have a defined crystalline cubic structure. However, when produced by microbial metabolic activity, they can occur as framboidal pyrite. Framboidal pyrite has an increased reactive surface area (Weisener and Weber 2010) which could affect the porosity and diffusive flux in the sediment. The H<sub>2</sub>S flux calculated for the anoxic incubations showed a decrease in flux over time, which suggests that H<sub>2</sub>S was not as easily diffused out into the water column and is being sequestered into the sediment.

### **2.3.2 Geochemical Phase Classification Using Two Methods to Quantify Microbial and Atmospheric Effects**

#### ***Biom mineralization (Sulfide) Characterization in Oxic and Anoxic Environments Using Scanning Electron Microscopy (SEM)***

A modal investigation of the iron and sulfur mineral phases for the abiotic and biotic conditions was performed using SEM particle analyses. The proportion of sulfur

and iron-bearing phases was determined from a total population of 1000 grains in which elemental ratios were defined. Particles with a high percentage of sulfur and iron were categorized as pyrite or potentially greigite, a precursor to pyrite framboids (Wilkin and Barnes 1997), and compared to the proportion of iron oxide particles. Based on the elemental analyses for each particle, a strong contrast between the proportion of iron and sulfur-rich (<10% total modal percentage) particles were observed in the biotic incubations compared to the abiotic under anoxic conditions (Figure 2.1). The proportion of sulfide particles observed in the biotic incubations (higher percentages of iron and sulfur) make up 4% of all the particles analyzed for the anoxic biotic incubations. SEM micrographs in Figure 2.1 show an aggregation of submicron microcrystals with a Fe:S ratio of 1:1. These measurements suggest the formation of monosulfides (e.g., Greigite, Mackinawite), which are precursors to pyrite formation and are known to be associated with microbial activity (Wilkin and Barnes 1997; Frankel 2003; Gadd 2010). These will most likely be replaced by pyrite if conditions persist and are formed from  $H_2S$ , which is produced by sulfosulfate reducing bacteria. (Wilkin and Barnes 1997). The chemical profiles suggest that  $H_2S$  is most likely being sequestered into aggregates of sulfide within the sediment. These particles in the abiotic incubation make up only 0.3% of the particles analyzed for the abiotic incubations and 1.8% from the initial top sediment sludge. This suggested that the microbes were vital in the formation of iron sulfides in storage environments. In the oxic condition, there were fewer particles with high sulfur concentrations for both biotic and abiotic incubations, though a large proportion had high iron concentration. These high iron, but low sulfur particles are most likely iron oxides.

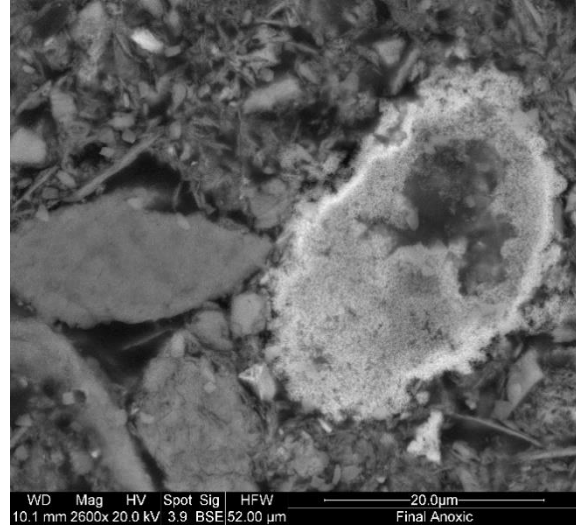
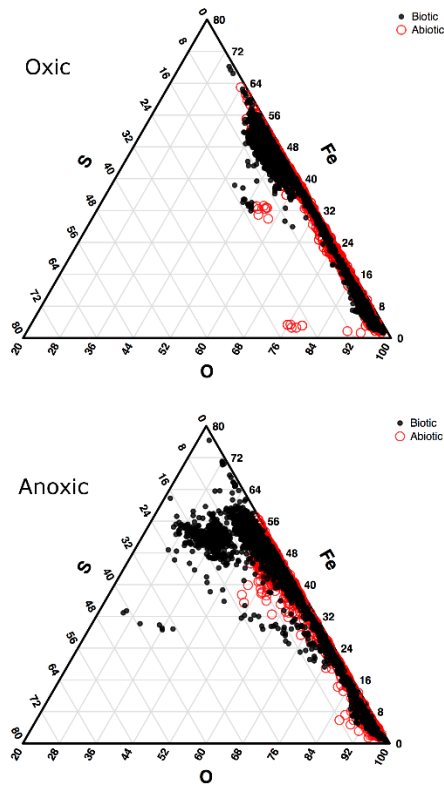


**Figure 2.1** SEM analysis of sludge collecting from final sediment samples; (a) Ternary plot shows the distribution of Fe, S, and O elemental concentrations. The oxic incubations are shown on the top figure and anoxic on the bottom, with data from the biotic incubations represented by solid black circles and the abiotic data represented by open red circles; (b) Example of a high sulfur and iron particle showing submicron microcrystals in a pre-framboidal texture.

## ***Solid Phase Characterization and Metal Behavior, Using Principal Component***

### ***Analyses (PCA)***

Five solid phase extractions (e.g., water soluble, amorphous oxyhydroxides, weakly bound iron oxide phases, those prone to biological complexations, and strong acid extractable) were used to target metal solubility within the sludge material as a function of treatment. The PCA along with ANOVA analyses determined which metals within each mineralogical phase were susceptible to either biotic or abiotic geochemical alteration in both the presence and absence of oxygen. Only the amorphous oxyhydroxide phase were susceptible to microbial effects, while the other four phases were more strongly affected by the presence or absence of oxygen, based on differences between oxic and anoxic incubations. Those four geochemical phases were not altered by the presence or absence of microbial activity e.g., no new secondary mineral phases produced (PCA scatterplots found in appendix).

The targeted amorphous oxyhydroxide phase (i.e., easily reducible) within the sludge was susceptible to both microbial and atmospheric effects based on a PCA analysis and ANOVA. Analyses of all four mesocosm conditions showed distinct variation as each reported to separate quadrants (Figure 2.2). 54% of the variance was explained by PC 1 and 27% of the variance was explained by PC 2, both of which are significant based on a 999-repetition row-wise bootstrap analysis. Both components had strong loadings from Fe, S, Al, and Ca with PC 2 suggesting an inverse relationship between Fe and S (figure of loadings found in appendix). Based on the scatter plot, it appears that PC2 shows microbial influence on the amorphous geochemical phase with the abiotic incubations both plotting positively, and the active incubations plotting negatively. The ANOVA

analysis supports this as well, showing a significant variance of Fe concentrations in this phase which suggests microbial and atmospheric effects. The Fe concentrations in this amorphous phase in the biotic oxic incubation ( $1400 \pm 300$  mg/kg) are approximately  $1.5\times$  greater than within the abiotic (concentrations found in appendix). These phases include amorphous iron oxyhydroxides such as ferrihydrite, which is commonly found in AMD environments and is associated with microbes (Ferris et al. 1989). Ferrihydrite can be formed directly by the oxidizing of Fe(II) by bacteria, or the bacteria can act as a nucleation site with mineralization of iron oxides encompassing both dead and living cells (Ferris et al. 1989). Since amorphous iron oxyhydroxides are also involved with the adsorption of trace metals (Gadde and Laitinen 1974; Tessier et al. 1985; Lee et al. 2002), an unstable environment for these mineral phases would cause other types of contaminants common in the mine to be released in addition to Fe.

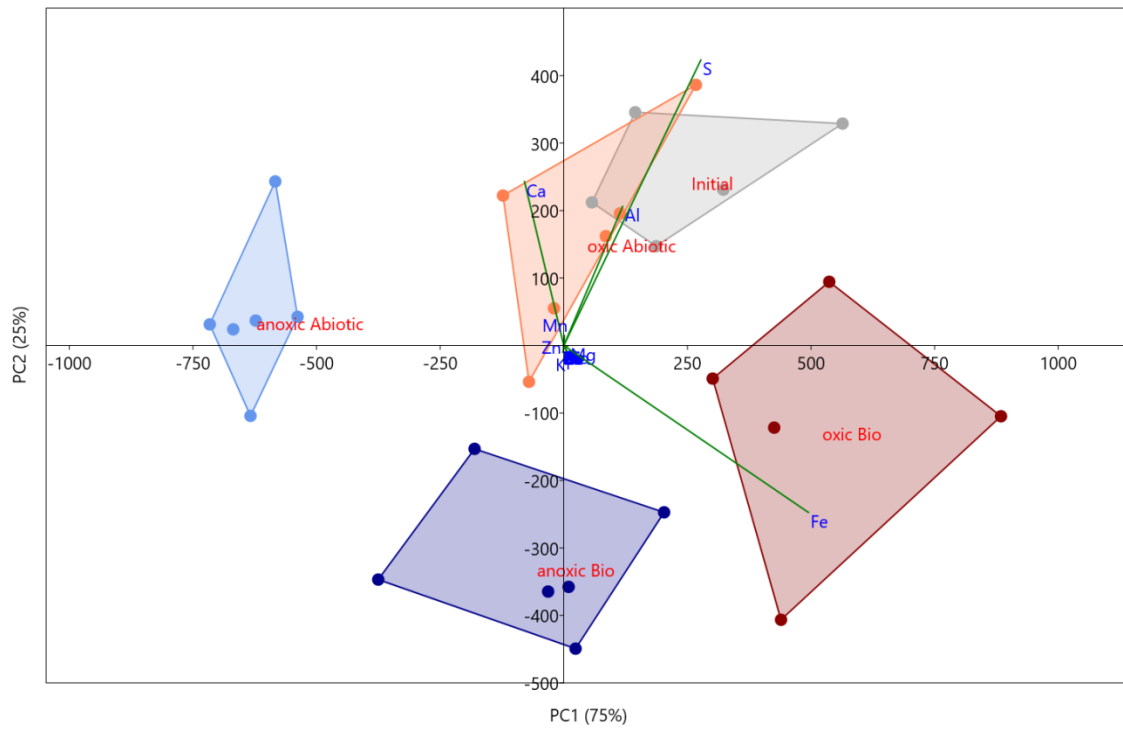


**Figure 2.2** PCA scatterplot for the Oxyhydroxide mineral phases in all four experimental conditions and the initial in situ sediment from the MSB. PC1 represents 77% of the variance, while PC2 represents 20%. Convex hulls are connecting sample groups labelled on the figure, generated in PAST.

Other targeted phases included organically bound, water soluble, metals weakly bound to oxides, and strong acid extractable (total metals) phases. All followed a similar trend, with the atmospheric effects having a greater influence than the microbial effects. The variation in these geochemical phases was based on both PCA and ANOVA. For these phases, PC 1 explains >90% of the variance, and apart from the water-soluble phase, they all had strong loadings of Fe. In the water-soluble phase, PC 1 had loadings of Ca, S, and Mn. Concentrations within water-soluble fractions were lower in the anoxic mesocosm compared to the oxic for S ( $150 \pm 15$  compared to  $250 \pm 15$  mg/kg) and Mn ( $10 \pm 1$  kg compared to  $40 \pm 5$  mg/kg). This suggested higher stability in anoxic conditions concerning possible contaminants such as Mn and S. Other contaminants such as Zn ( $\sim 0.2$  mg/kg) and Mg ( $\sim 25$  mg/kg) were not significantly different between atmospheric effects, and Fe is not contained within any water-soluble phases. Compared to Mn and S, Zn, Mg, and Fe had no impact on the stability of the sediment based on the water-soluble phases.

The organically bound, weakly bound to oxides, and strong acid extractable phases all had strong loadings of Fe. The organically bound Fe concentration in the oxic mesocosm was  $90 \pm 20$  (abiotic) and  $210 \pm 70$  mg/kg (biotic) with no significant difference between abiotic and biotic in the anoxic conditions ( $2300 \pm 300$  mg/kg). Under anoxic conditions, Fe(II) will form colloids with organic matter and may be mobile in organic-rich systems based on a laboratory study (Liao et al. 2017). In a typical AMD or mine environment, organic matter may not be high, but previous studies suggest that mixing with soils under anoxic conditions may increase the chance of stable colloid formations, which may be easily transported downstream (Wilkin et al. 1997). Iron was

not contained in the weakly bound oxides phase in the anoxic mesocosm, though the oxic had  $2700 \pm 200$  mg/kg in the biotic and slightly less ( $2200 \pm 300$  mg/kg) for the abiotic. There were fewer oxides in the anoxic mesocosm overall, and iron may be preferentially adsorb to organic matter in the anoxic condition, rather than any oxides present.

Although Zn did not have strong loadings in any of the geochemical phases tested based on the PCAs, it is identified as an element of concern for the mine. Based on this study, up to  $33 \pm 5$  mg/kg of zinc could be in the initial sediment across all mineral phases, though this decreases to 21-27 mg/kg after all incubations, suggesting that some Zn was possibly unaccounted for in the extractions or went under dissolution into the water column. Besides total extractable metals, the highest concentration of Zn was found in the extraction targeting sorbed metals to poorly crystalline phases, which was found to vary significantly by atmospheric condition ( $17 \pm 4$  mg/kg in the oxic and between 4–7 mg/kg in the anoxic). Zn will most likely be adsorbed or coprecipitated with oxyhydroxides (Gadde and Laitinen 1974; Tessier et al. 1985; Lee et al. 2002) in the oxic mesocosm. In this case Zn will be insoluble in water, based on the soluble phase phases' extractions ( $<0.5$  mg/kg measured). Other mineral phases had concentrations of zinc less than 2 mg/kg with no significant microbial or atmospheric effects.

### **2.3.3 Community Structure Shifts as a Function of Anoxic and Oxic Incubation Environments**

To determine correlated factors controlled by microbial effects, 59 samples were analyzed for the microbial community, detecting over 500,000 quality sequences with an average of 8793 sequences per sample. Sequences within samples ranged from 3000–20,294 (after a low-read cut-off) and were clustered into 14,489 OTUs. Between the oxic



and anoxic communities, there were 137 OTUs out of 14,489 OTUs identified as significantly differentially abundant (adjusted p-value less than 0.05). The majority of these OTUs (97/137) are highly abundant in the oxic incubations and represent 18.3% of the normalized (DeSEQ2) sequence counts. The OTUs that are overrepresented in the anoxic incubations represent 8.7% of the normalized sequence counts from samples in the anoxic time point. Rarefaction was completed on samples with over 3000 sequence hits at 10 iterations to determine species richness. Curves produced did not completely plateau, suggesting that full coverage was not reached, though for many samples it appeared to be close (curves found in appendix). Shannon and Chao1 indices were used to determine microbial diversity using the rarefaction cut-off of 3000. Diversity was slightly higher in the oxic incubations compared to the anoxic atmospheric environments, though neither were significantly different from the initial sediment (Table 2.3).

A PCoA suggested a community shift for both oxic and anoxic communities (Figure 2.3). All samples that were incubated plotted in the positive quadrants of PC 1 & 2 with samples from months 3 and 5 overlapping for both oxic and anoxic mesocosm. The final timepoints plotted separately and suggested a shift in the community later in the incubation that created a more unique community for the anoxic mesocosm. For this reason, the rest of the results will focus on the final timepoints to determine major long-term differences in the microbial community for oxic and anoxic storage. This will also allow for direct comparisons to geochemical phases as these were collected at the end of the incubations.

**Table 2.3** Alpha rarefaction showing average diversity metrics for the time points of each incubation with the standard deviation between the replicates and the iterations shown.

	Months	Chao	Shannon	Observed Rarefied OTUs
	Initial	2065 $\pm$ 200	7.5 $\pm$ 0.2	930 $\pm$ 50
anoxic	1	2199 $\pm$ 100	7.71 $\pm$ 0.03	960 $\pm$ 10
	3	2184 $\pm$ 300	7.4 $\pm$ 0.5	920 $\pm$ 100
	5	1479 $\pm$ 60	7.5 $\pm$ 0.4	810 $\pm$ 100
oxic	1	2618 $\pm$ 100	8.2 $\pm$ 0.1	1130 $\pm$ 40
	3	2243 $\pm$ 200	7.7 $\pm$ 0.1	960 $\pm$ 40
	5	1732 $\pm$ 200	7.6 $\pm$ 0.3	850 $\pm$ 100

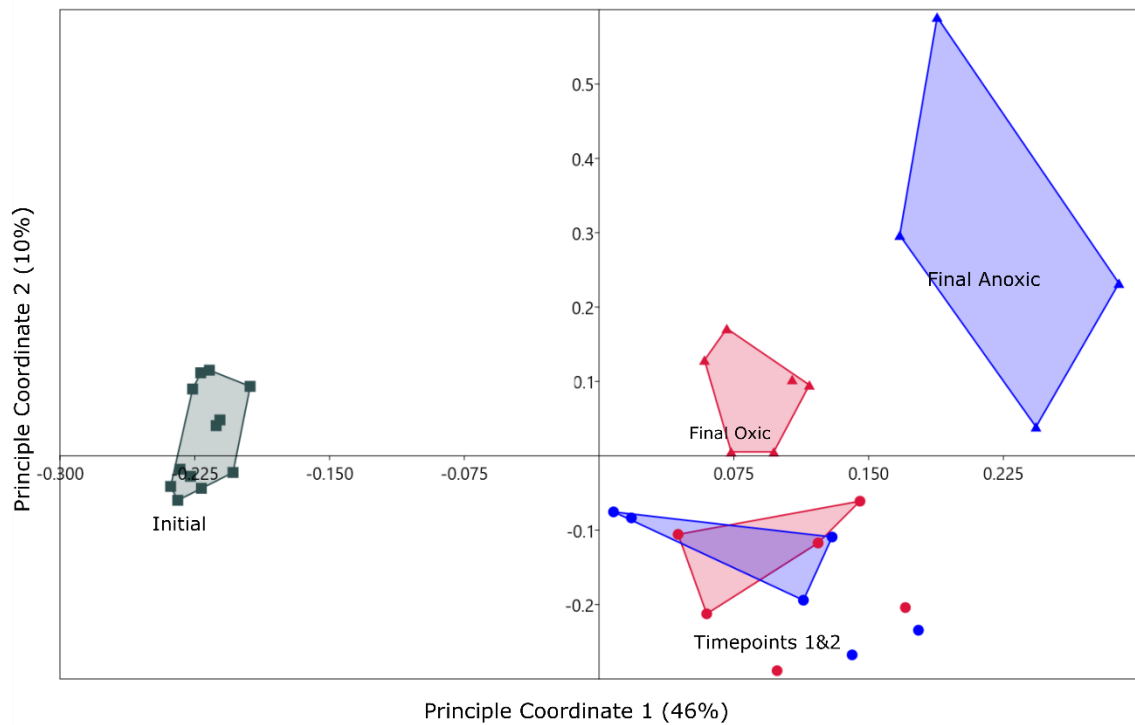


**Figure 2.3** PCoA of the top 1000 OTUs from the initial (squares), oxic (red) and anoxic (blue) incubations. Final timepoints (month 5) are represented by triangles for both atmospheric conditions. Coordinate one represents 46% of the variance and coordinate two represents 10%. Convex hulls are connecting sample groups on the figure, done within PAST. Timepoints one and two represent month 1 and 3 sampling periods.

PCoA suggested a shift from the initial community in the bioreactor based on an input of OTUs which needed to be classified into taxonomic groups in order to put context into the changes observed. OTUs in the initial samples were identified to be from the following phyla: *Proteobacteria* (40%), unassigned (12%), *Acidobacteria* (12%), *Chloroflexi* (5%), *Planctomycetes* (5%), and *Actinobacteria* (5%), with other groups making up the remaining 21% and individually less than 5%. After incubation in an oxic condition, the community was similar to the initial community when looking at the distribution of phyla. Sequences were identified to *Proteobacteria* (30%), *Acidobacteria* (13%), *Bacteroidetes* (9%), unassigned (9%), *Chloroflexi* (6%), and *Actinobacteria* (6%) phyla and other groups contributing individually less than 5%. Sequences in the anoxic community sequences are divided into *Proteobacteria* (30%), *Firmicutes* (16%), *Bacteroidetes* (12%), unassigned (10%), *Acidobacteria* (6%), and *Chloroflexi* (4%). From a phylum perspective, the oxic mesocosm is closer to the initial community than the anoxic, apart from *Bacteroidetes* which increased in both oxic and anoxic mesocosms. The anoxic community was found to have an abundance of *Firmicutes*, which were initially below 5% in the MSB.

Based on the analysis of phyla alone, certain aspects appear unchanged by storage in anoxic conditions, specifically the *Proteobacteria* community. In initial, oxic, and anoxic mesocosms *Proteobacteria* is the dominant phylum, though after incubation the taxonomic classification at the Class level suggests a shift in the proteobacteria community related to atmospheric conditions. The top 15 classes (representing 70–80% of the normalized sequences), included *Gammaproteobacteria*, and *Alphaproteobacteria* which are abundant in the initial MSB community (20% and 11% respectively) with low

abundance of *Deltaproteobacteria* (Figure 2.4). The oxic mesocosms appeared to be somewhat similar in composition to the initial, although the overall abundance of classes within *Proteobacteria* decreased. The anoxic community saw a large shift from a dominantly *Proteobacteria* community, to a more *Deltaproteobacteria* dominant community. Another class that was dominant within the anoxic community is *Clostridia* (*Firmicutes*), which was less than 1% of the initial community. OTUs that were identified as differentially abundant were also classified into *Deltaproteobacteria* and *Clostridia*, suggesting that both groups were unique to the anoxic mesocosm compared to the oxic, and may have impacted the geochemistry.

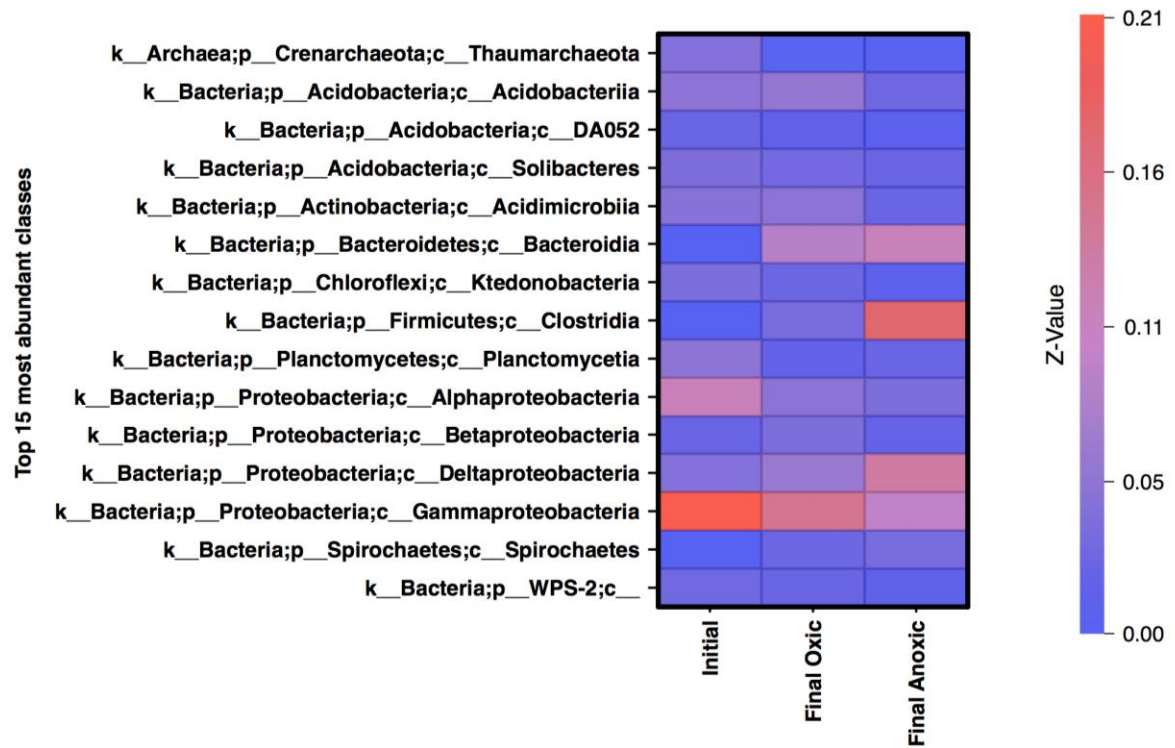


**Figure 2.4** Heatmap of the relative abundance of normalized counts for the top 15 most abundant classes in the final timepoints and the initial samples with the relative abundance displayed on the y-axis, normalized to 1 for the total community. Most abundant classes are shown in red while the least abundant are shown in blue.

#### **2.3.4 Biogeochemical Connections of AMD Sludge, and Associated Risks**

To correlate the geochemical phases and the microbial community drivers for the biotic incubations, a CCA analysis was performed using the PC loadings from each geochemical phase (Figure 2.5). For all phases, except for the amorphous oxyhydroxide phase, only PC 1 was used as others were insignificant. Based on this CCA, PC 2 of the oxyhydroxide phase correlates with the community in the oxic condition. PC 2 had strong loadings of Fe, with a negative correlation to S, and based on the PCA scatterplot (Figure 2.2), controls the variance associated with the effects of microbes on this phase. Fe was sequestered in the sediment during incubation by microbes in the oxic phase, while mechanisms for sulfur sequestration in an oxic condition are unlikely at this pH and temperature. The bioavailable phase appears to correlate with microbial activity based on this CCA plot, however, based on the concentrations of Fe in this phase there is no significant difference between the biotic and abiotic incubations. Fe may be bound to organic substances that were already present in the sediment such as organic material from the mussel shells and not affected by active microbes. All other phases do not appear to correlate to the three groups, which is supported by the PCA results, in that no biological effects were found for those phases.

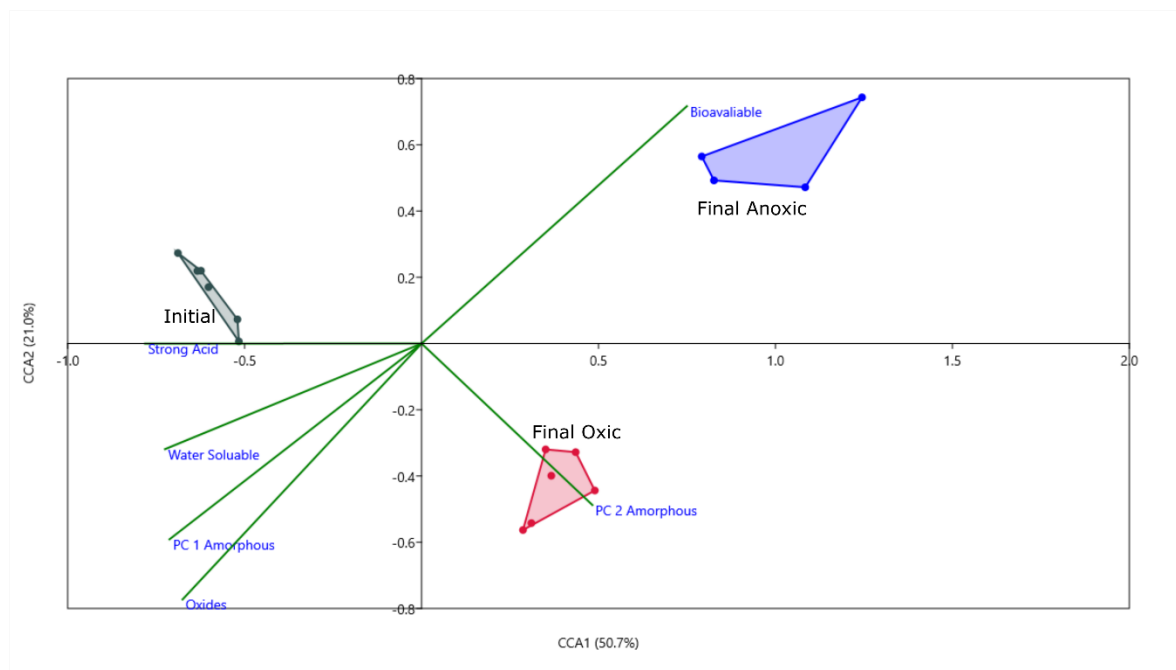


**Figure 2.5** CCA plot using PCA components as environmental variables for each geochemical phase. PC 1 and PC 2 are included for the oxyhydroxide mineral phase as they are both significant, and only PC 1 is included for all other phases. Axis one represents 50% of the variance and axis 2 represents 21%. Convex hulls are connecting sample groups on the figure, done within PAST.



Based on the PCA, CCA, and particle analysis presented, there are significant geochemical differences based on oxic or anoxic incubation. Some of these differences can be attributed to microbial activity (observed microbial effects), such as the increased Fe in oxyhydroxide phases and counts of particles with high sulfur content (possible Greigite). For this reason, differential abundance was used to tease out differences between the oxic and anoxic community on an OTU level and to identify important groups that influenced geochemistry in each environment. Genera which are significantly differentially abundant in oxic and anoxic, and highly abundant in the initial MSB for comparison were shown in Figure 2.6.

Within the oxic incubation, OTUs classified as unidentified genera within the families of *Xanthomonadaceae*, *Acidimicrobiales*, *Ignavibacteriaceae*, and *Porphyromonadaceae* (*Plaudibacter*) were significantly differentially abundant compared to the anoxic environments. These differentially abundant groups may have been responsible for the further oxidation and increased production of amorphous iron oxyhydroxides as noted by the geochemical phase extractions and correlations based on the CCA plot (Figure 2.5). The family *Acidimicrobiales*, in particular, may have included the iron oxidizing species such as *Acidimicrobium ferrooxidans* (Clark and Norris 1996), which could have been responsible for increased iron oxide production. Other highly abundant bacteria such as *Pseudomona* and *Bacteroidales* present in the incubation could be responsible for organic carbon degradation or act as a nucleation site for mineralization of hydroxides (Ferris et al. 1989). Iron oxides are insoluble in most neutral waters but could dissolve if in acidic environments (Schwertmann 1991). In previous studies, acidic environments were shown to cause dissolution of AMD sludge and

suggested soil mixing or a protective gravel layer (Demers et al. 2015; Demers et al. 2017). The ability for the sludge to act as an oxygen barrier was also tested in this previous study which found a varying oxygen flux from 0–50 mmol m<sup>-2</sup> day<sup>-1</sup> over a period of two years in a column experiment. This study suggested that AMD sludge with low oxygen flux (<20) could be used as an oxygen barrier for other mine tailings or waste rock with soil mixing and water cover (Demers et al. 2015; Demers et al. 2017). Oxygen flux in this study remained stable with microbial activity, suggesting that this form of management is a possibility, if the probability of metal dissolution is low, and will not contribute to AMD. Another possible issue with AMD remediation sludge being used as an oxygen barrier is the potential for the sediment to dry and crack, which would cause preferential pathways for oxygen-rich waters to travel (Zinck and Griffith 2005). A solution to this, as noted by Zinck and Griffith (2005), is to apply either a vegetation cover or a water cap so that the sludge/sediment remains saturated.

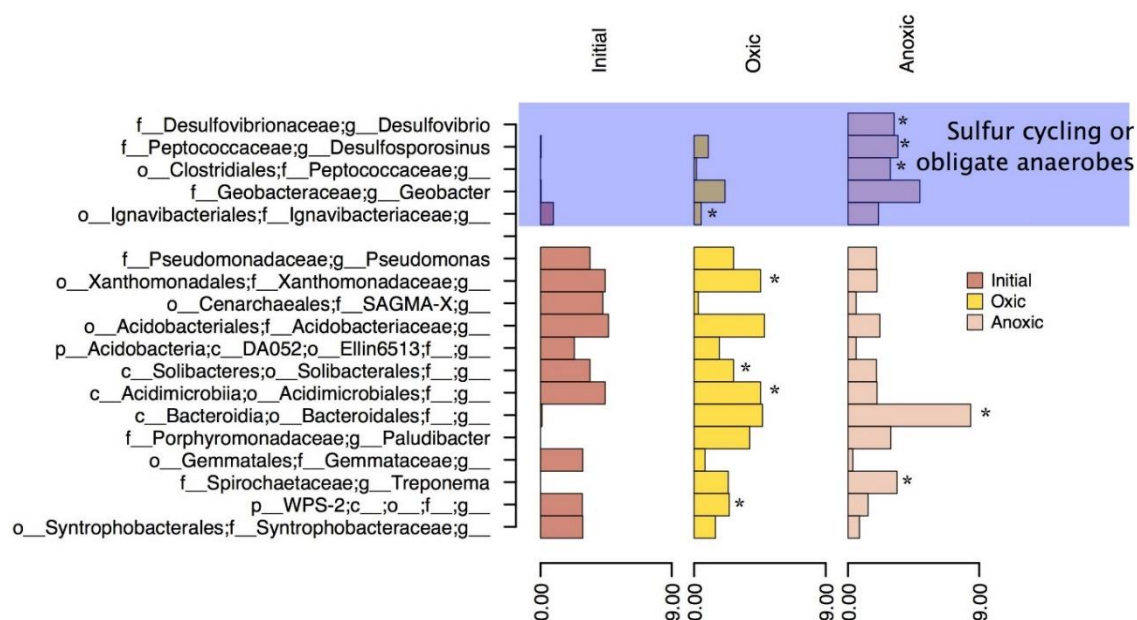


**Figure 2.6** Most abundant Genera in the final oxidic and anoxic timepoints, as well as the initial in situ bacteria. The asterisks represent genera that have significant differential abundant OTUs between the oxidic and anoxic communities. The top blue section of the figure are Genera that have shown to be important for sulfur cycling or other obligate anaerobic pathways based on literature searches.

Differential abundant OTUs in the anoxic mesocosms were identified most commonly in the *Desulovibrio* and *Desulfosporosinus* genus (within *deltaproteobacteria* and *clostridia* classes respectively). The MSB sludge in this study showed a comparable increase in particles with high iron and sulfur concentrations after anoxic incubation which correlates to the abundant genera of SRB's observed. Genera such as *Desulovibrio* and *Desulfosporosinus* are abundant in this system (Figure 2.6) and can reduce sulfate using a dissimilatory reduction pathway to produce H<sub>2</sub>S. These genera have been found in both AMD (Barton and Hamilton 2007; Schippers et al. 2010b; Sánchez-Andrea et al. 2014; Florentino et al. 2015; Méndez-García et al. 2015) and AMD remediation environments (Lee et al. 2009) in previous studies and are most likely responsible for the sulfide microcrystallites observed in the anoxic biotic incubations. For these reactions to occur there would have to be a source of low molecular weight organic carbon usually formed by the degradation of more complex molecules. The source of carbon in this system would most likely be from organic material and chitin left behind in shell fragments that would be inadvertently collected when removing the sediment/sludge layer. Bacteria such as *Pseudomonas* (5% of the sequences) could be responsible for the degradation of carbon, suggested by their high abundance in the current system and high metabolic diversity allowing them to survive in AMD environments (Wakeman et al. 2010; Martins et al. 2011; Sánchez-Andrea et al. 2014; Bruneel et al. 2017). *Pseudomonas* has been previously suggested to live in combination with SRB's within the deeper (and anoxic) sections of the MSB (Falk et al. 2018). The anoxic incubation provided a way to test if the microbial community from the oxic portion of the bioreactor could thrive in an anoxic environment and if they increased the stability of the sediment/sludge in this environment. Since SRB's were present, and H<sub>2</sub>S was produced

and reacted to form a precursor to pyrite framboids, the microbes would cause an increased stability with regard to metal contamination if the sediment was placed in an anoxic environment, such as deep-pit burial. Anoxic zones are a more traditional method of storing mine wastes, either in the form of stockpiles or tailings ponds. Stockpiles can be effective if planned correctly, and currently are being used for waste rock storage on the mine site in this study.

## **2.4 Conclusions**

Mussel shell bioreactors are an effective and inexpensive way to remediate AMD; however, depending on the area of their deployment, there is the potential for gradual accumulation of a sludge layer. The accumulation of sediment (e.g., alluvium and aeolian deposition) on the surface of the bioreactor is a limiting factor and requires management. AMD sludge management requires risk assessment of this secondary contamination for assessment of metal release and provides added information on whether the material can be actively repurposed. In this study, both anoxic and oxic storage mechanisms were investigated to evaluate the microbial impacts on the material. Storage of the sludge residue under oxic conditions increased soluble Mn, Al, and S phases. The presence of bacteria had a significant impact on the release of metals associated with oxyhydroxide mineral phases. These bacteria were an underlying factor in the low sediment oxygen demand (SOD) which resulted in steady state control of oxygen flux into the sediment. Although this material may be useful as an oxygen barrier over tailings or waste rock, there is still the possibility of metals being remobilized. Based on the results of this study, current repurposing of this AMD sludge should be applied to saturated circumneutral environments (e.g., wetlands, backfills, or under soil caps). These conclusions were

further supported while investigating the stability of this material under anoxia. Storage of sludge material under anoxic conditions promotes the formation of iron sulfides, which immobilized the metals of concern at this location. Microbial community analyses indicated the presence of active SRB communities. This was further correlated with chemical measurements which showed measurable  $H_2S$  within the laboratory mesocosms associated with a shift in microbial community structure. Under conditions of anoxia, further evidence of increased metals associated with stable organic phases was also apparent. From a procedural perspective, burial mitigation may be the best solution to manage the AMD sludge.

## 2.5 References

- Akcil A, Koldas S (2006) Acid Mine Drainage (AMD): causes, treatment and case studies. *J Clean Prod* 14:1139–1145. doi: 10.1016/j.jclepro.2004.09.006
- Aria Amirbahman \*, René Schönenberger, C. Annette Johnson and, Sigg L (1998) Aqueous- and Solid-Phase Biogeochemistry of a Calcareous Aquifer System Downgradient from a Municipal Solid Waste Landfill (Winterthur, Switzerland). doi: 10.1021/ES970810J
- Armitage PD, Bowes MJ, Vincent HM (2007) Long-term changes in macroinvertebrate communities of a heavy metal polluted stream: the river Nent (Cumbria, UK) after 28 years. *River Res Appl* 23:997–1015. doi: 10.1002/rra.1022
- Barton LL, Hamilton A (2007) *The Sulphate-Reducing Bacteria*. Cambridge University Press, New York
- Boudens R, Reid T, VanMensel D, et al (2016) Bio-physicochemical effects of gamma irradiation treatment for naphthenic acids in oil sands fluid fine tailings. *Sci Total Environ* 539:114–124. doi: 10.1016/J.SCITOTENV.2015.08.125
- Bridge G (2004) CONTESTED TERRAIN: Mining and the Environment. *Annu Rev Environ Resour* 29:205–259. doi: 10.1146/annurev.energy.28.011503.163434
- Bruneel O, Mghazli N, Hakkou R, et al (2017) In-depth characterization of bacterial and archaeal communities present in the abandoned Kettara pyrrhotite mine tailings (Morocco). *Extremophiles* 21:671–685. doi: 10.1007/s00792-017-0933-3
- Chao A (1984) Nonparametric Estimation of the Number of Classes in a Population. *Scand. J. Stat.* 11:265–270.
- Chen M, Walshe G, Chi Fru E, et al (2013) Microcosm assessment of the biogeochemical development of sulfur and oxygen in oil sands fluid fine tailings. *Appl Geochemistry* 37:1–11. doi: 10.1016/J.APGEOCHEM.2013.06.007
- Clark DA, Norris PR (1996) *Acidimicrobium ferrooxidans* gen. nov., sp. nov.: mixed-culture ferrous iron oxidation with *Sulfobacillus* species. *Microbiology* 142:785–790. doi: 10.1099/00221287-142-4-785
- Demers I, Benzaazoua M, Mbonimpa M, et al (2015) Valorisation of acid mine drainage treatment sludge as remediation component to control acid generation from mine wastes, part 1: Material characterization and laboratory kinetic testing. *Miner Eng* 76:109–116. doi: 10.1016/j.mineng.2014.10.015
- Demers I, Mbonimpa M, Benzaazoua M, et al (2017) Use of acid mine drainage treatment sludge by combination with a natural soil as an oxygen barrier cover for mine waste reclamation: Laboratory column tests and intermediate scale field tests. *Miner Eng* 107:43–52. doi: 10.1016/j.mineng.2016.11.017
- DiLoreto ZA, Weber PA, Olds W, et al (2016a) Novel cost effective full scale mussel shell bioreactors for metal removal and acid neutralization. *J Environ Manage.* doi: 10.1016/j.jenvman.2016.09.023

- DiLoreto ZA, Weber PA, Weisener CG (2016b) Solid phase characterization and metal deportment in a mussel shell bioreactor for the treatment of AMD, Stockton Coal Mine, New Zealand. *Appl Geochemistry* 67:133–143. doi: 10.1016/j.apgeochem.2016.02.011
- Edgar RC (2010) Search and clustering orders of magnitude faster than BLAST. *Bioinformatics* 26:2460–2461. doi: 10.1093/bioinformatics/btq461
- Edgar RC, Haas BJ, Clemente JC, et al (2011) UCHIME improves sensitivity and speed of chimera detection. *Bioinformatics* 27:2194–2200. doi: 10.1093/bioinformatics/btr381
- Falk N, Chaganti SR, Weisener CG (2018) Evaluating the microbial community and gene regulation involved in crystallization kinetics of ZnS formation in reduced environments. *Geochim Cosmochim Acta* 220:201–216. doi: 10.1016/J.GCA.2017.09.039
- Fangueiro D, Bermond A, Santos E, et al (2002) Heavy metal mobility assessment in sediments based on a kinetic approach of the EDTA extraction: Search for optimal experimental conditions. *Anal Chim Acta* 459:245–256. doi: 10.1016/S0003-2670(02)00134-4
- Ferris FG, Tazaki K, Fyfe WS (1989) Iron oxides in acid mine drainage environments and their association with bacteria. *Chem Geol* 74:321–330. doi: 10.1016/0009-2541(89)90041-7
- Florentino AP, Weijma J, Stams AJM, Sánchez-Andrea I (2015) Sulfur Reduction in Acid Rock Drainage Environments. *Environ Sci Technol*. doi: 10.1021/acs.est.5b03346
- Frankel RB (2003) Biologically Induced Mineralization by Bacteria. *Rev Mineral Geochemistry* 54:95–114. doi: 10.2113/0540095
- Gadd GM (2010) Metals, minerals and microbes: Geomicrobiology and bioremediation. *Microbiology* 156:609–643. doi: 10.1099/mic.0.037143-0
- Gadde RR, Laitinen HA (1974) Studies of Heavy Metal Adsorption by Hydrous Iron and Manganese Oxides. *Anal Chem* 46:2022–2026. doi: 10.1021/ac60349a004
- Han Y-S, Youm S-J, Oh C, et al (2017) Geochemical and eco-toxicological characteristics of stream water and its sediments affected by acid mine drainage. *CATENA* 148:52–59. doi: 10.1016/J.CATENA.2015.11.015
- Heron G, Christensen TH, Tjell JC (1994) Oxidation Capacity of Aquifer Sediments. *Environ Sci Technol* 28:153–158. doi: 10.1021/es00050a021
- Lee G, Bigham JM, Faure G (2002) Removal of trace metals by coprecipitation with Fe, Al and Mn from natural waters contaminated with acid mine drainage in the Ducktown Mining District, Tennessee. *Appl Geochemistry* 17:569–581. doi: 10.1016/S0883-2927(01)00125-1
- Lee Y-J, Romanek CS, Wiegel J (2009) *Desulfosporosinus youngiae* sp. nov., a spore-forming, sulfate-reducing bacterium isolated from a constructed wetland treating



- acid mine drainage. *Int J Syst Evol Microbiol* 59:2743–2746. doi: 10.1099/ij.s.0.007336-0
- Liao P, Li W, Jiang Y, et al (2017) Formation, Aggregation, and Deposition Dynamics of NOM-Iron Colloids at Anoxic–Oxic Interfaces. *Environ Sci Technol* 51:12235–12245. doi: 10.1021/acs.est.7b02356
- Lloyd M, Ghelardi RJ (1964) A Table for Calculating the 'Equitability' Component of Species Diversity. *J Anim Ecol* 33:217. doi: 10.2307/2628
- Love MI, Huber W, Anders S (2014) Moderated estimation of fold change and dispersion for RNA-seq data with DESeq2. *Genome Biol* 15:550. doi: 10.1186/s13059-014-0550-8
- Macías F, Pérez-López R, Caraballo MA, et al (2017) Management strategies and valorization for waste sludge from active treatment of extremely metal-polluted acid mine drainage: A contribution for sustainable mining. *J Clean Prod* 141:1057–1066. doi: 10.1016/J.JCLEPRO.2016.09.181
- Martins M, Faleiro ML, Silva G, et al (2011) Dynamics of bacterial community in up-flow anaerobic packed bed system for acid mine drainage treatment using wine wastes as carbon source. *Int Biodeterior Biodegrad* 65:78–84. doi: 10.1016/j.ibiod.2010.09.005
- Mayes WM, Johnston D, Potter HAB, Jarvis AP (2009) A national strategy for identification, prioritisation and management of pollution from abandoned non-coal mine sites in England and Wales. I.: Methodology development and initial results. *Sci Total Environ* 407:5435–5447. doi: 10.1016/J.SCITOTENV.2009.06.019
- McCauley C, O'Sullivan A, Weber P, Trumm D (2010) Variability of Stockton Coal Mine drainage chemistry and its treatment potential with biogeochemical reactors. *New Zeal J Geol Geophys* 53:211–226. doi: 10.1080/00288306.2010.503565
- McCauley C, O'Sullivan AD, Weber P, Trumm D (2009a) Stockton Mine Acid Mine Drainage and Its Treatment using Waste Substrates in Biogeochemical Reactors.
- McCauley CA, O'Sullivan AD, Milke MW, et al (2009b) Sulfate and metal removal in bioreactors treating acid mine drainage dominated with iron and aluminum. *Water Res* 43:961–970. doi: 10.1016/j.watres.2008.11.029
- Méndez-García C, Peláez AI, Mesa V, et al (2015) Microbial diversity and metabolic networks in acid mine drainage habitats. *Front. Microbiol.* 6:
- Nordstrom DK (1985) The rate of ferrous iron oxidation in a stream receiving acid mine effluent. *Sel Pap Hydrol Sci* 113–119.
- Parada AE, Needham DM, Fuhrman JA (2016) Every base matters: assessing small subunit rRNA primers for marine microbiomes with mock communities, time series and global field samples. *Environ Microbiol* 18:1403–1414. doi: 10.1111/1462-2920.13023

- Pope J, Weber P, Mackenzie A, et al (2010) Correlation of acid base accounting characteristics with the Geology of commonly mined coal measures , West Coast and Southland , New Zealand. doi: 10.1080/00288306.2010.498404
- Reid T, Boudens R, Ciborowski JJH, Weisener CG (2016) Physicochemical gradients, diffusive flux, and sediment oxygen demand within oil sands tailings materials from Alberta, Canada. *Appl Geochemistry* 75:90–99. doi: 10.1016/J.APGEOCHEM.2016.10.004
- Revsbech NP (1989) Diffusion characteristics of microbial communities determined by use of oxygen microsensors. *J Microbiol Methods* 9:111–122. doi: 10.1016/0167-7012(89)90061-4
- Revsbech NP, Nielsen LP, Ramsing NB (1998) A novel microsensor for determination of apparent diffusivity in sediments. *Limnol Oceanogr* 43:986–992. doi: 10.4319/lo.1998.43.5.0986
- Ribeta I, Ptacek CJ, Blowes DW, Jambor JL (1995) The potential for metal release by reductive dissolution of weathered mine tailings. *J Contam Hydrol* 17:239–273. doi: 10.1016/0169-7722(94)00010-F
- Sánchez-Andrea I, Sanz JL, Bijmans MFM, Stams AJM (2014) Sulfate reduction at low pH to remediate acid mine drainage. *J Hazard Mater.* doi: 10.1016/j.jhazmat.2013.12.032
- Schippers A, Breuker A, Blazejak A, et al (2010) The biogeochemistry and microbiology of sulfidic mine waste and bioleaching dumps and heaps, and novel Fe(II)-oxidizing bacteria. *Hydrometallurgy* 104:342–350. doi: 10.1016/j.hydromet.2010.01.012
- Schippers A, Jozsa P-G, Sand W (1998) Evaluation of the efficiency of measures for sulphidic mine waste mitigation. *Appl Microbiol Biotechnol* 49:698–701. doi: 10.1007/s002530051234
- Schwertmann U (1991) Solubility and dissolution of iron oxides. *Plant Soil* 130:1–25. doi: 10.1007/BF00011851
- Singer PC, Stumm W (1970) Acidic Mine Drainage: The Rate-Determining Step. *Source Sci New Ser* 167:1121–1123.
- Tessier A, Rapin F, Carignan R (1985) Trace metals in oxic lake sediments: possible adsorption onto iron oxyhydroxides. *Geochim Cosmochim Acta* 49:183–194. doi: 10.1016/0016-7037(85)90203-0
- Thorbergsdóttir IM, Reynir Gíslason S, Ingvason HR, Einarsson Á (2004) Benthic oxygen flux in the highly productive subarctic Lake Myvatn, Iceland: In situ benthic flux chamber study. *Aquat Ecol* 38:177–189. doi: 10.1023/B:AECO.0000032057.95464.ad
- Trumm D, Ball J, Pope J, Weisener C (2015) Passive Treatment of ARD Using Mussel Shells – Part III : Technology Improvement and Future Direction. 10th Int Conference Acid Rock Drain IMWA Conf 1–9.

- Wakeman KD, Erving L, Riekkola-Vanhanen ML, Puhakka JA (2010) Silage supports sulfate reduction in the treatment of metals- and sulfate-containing waste waters. *Water Res* 44:4932–4939. doi: 10.1016/j.watres.2010.07.025
- Weisener C, Weber P (2010) Preferential oxidation of pyrite as a function of morphology and relict texture. *New Zeal J Geol Geophys* 53:167–176. doi: 10.1080/00288306.2010.499158
- Weiss S, Xu ZZ, Peddada S, et al (2017) Normalization and microbial differential abundance strategies depend upon data characteristics. *Microbiome* 5:27. doi: 10.1186/s40168-017-0237-y
- Wilkin RT, Barnes HL (1997) Formation processes of framboidal pyrite. *Geochim Cosmochim Acta* 61:323–339. doi: 10.1016/S0016-7037(96)00320-1
- Zinck J, Griffith W (2005) CANMET Mining and Mineral Sciences Laboratories. *Mine Environ Neutral Drain* 1–60.
- (2017) Unisense A/S. In: Unisense A/S.

## **Chapter 3**

### **Summary of Mussel shell bioreactor sludge using field leaching columns as a comparison to laboratory mesocosms**

#### **3.1 Introduction**

A novel full-scale bioreactor currently being studied at an active coal mine in New Zealand is using waste mussel shells as a cheap alternative to traditional alkaline materials (McCauley et al. 2009b; Uster et al. 2014; Trumm et al. 2015; DiLoreto et al. 2016a). These shells have a high neutralizing capacity and contain enough organic matter (both chitin and residual “meat”) to promote the growth of sulfur reducing bacteria (SRB). The mussel shell bioreactor (MSB) is currently treating an AMD seep at the Stockton coal mine on the west coast of the South Island of New Zealand, an area with a history of coal mining and AMD-impacted freshwater streams. The coal mine is located on the Brunner Coal measures with a lithology of coal and marine mudstones containing up to 5 wt% pyrite, with lesser carbonates providing little opportunity for natural neutralization of AMD (Pope et al. 2010; Weisener and Weber 2010). Seeps within the mine have been found to have high levels of Fe and Al (98% of metal loadings) as well as Cu, Ni, Mn, Zn, Pb, Cd, and As (McCauley et al. 2010).

The ability of the MSB to treat AMD has decreased since its first installation in 2012, primarily due to a layer of low permeability sludge that has settled on top of the reactor. This sludge has been removed to promote water flow into the mussel shells which is where remediation occurs. The sludge layer is potentially acid forming (PAF), with a pH of 3-4, and contains minerals such gibbsite (an aluminum hydroxide), and ferrierite

(zeolite mineral that is often porous and impure) (DiLoreto et al. 2016b). This material poses potential risks of metals associated with this sludge to be remobilized and must be stored in a way that avoids these risks. The MSB has been installed since 2012 and the sludge layer has caused the reactor to fail after only about 5 years of operation. Without the sludge layer the lifespan of the reactor is currently unknown and the main factor controlling this would be the amount of calcium carbonate which has been reacted. Based on the amount of calcium carbonate currently in the reactor compared to when it was installed, the longevity of the MSB can be estimated. Estimates were made based on the presence and (theoretical) absence of the sludge layer to determine the length of time the reactor could last if the sludge layer was not impeding the flow.

In this study the geochemical effects of storage on AMD sludge were determined using field leaching columns. The first goal of this field study is to be used in combination with previous lab studies (Butler et al. 2019) to compare and corroborate the simulated burial environments with field data. Physicochemical properties such as flux, and metals associated with geochemical phases were analysed, to further understand the risks associated with storage of the sludge under a dynamic environment. Field experiments are useful in combination with laboratory studies as they investigate *in situ* environmental factors relevant to this study, such as rainfall. The concentrations of metals leaching out of the sludge due to rainfall will provide important information for management purposes. To help determine which phases are most susceptible to dissolution by rainfall, geochemical phase extractions were done on the sludge after more than one year of leaching. A second goal of this study is to determine the estimates for longevity based on calcium dissolution rates of the MSB. Using this data, this chapter

aims to combine research from previous labs studies, field studies, and hydrological longevity predictions in order to review the use of MSB's.

## **3.2 Methods**

### **3.2.1 Experimental Design**

The field experiments consisted of two weathering stations in the bottom of clean 55 gallon barrels (polypropylene), located on the mine site. The volume of material was around 0.036 m<sup>3</sup> and estimated to 29kg of dry sludge. The columns were designed to investigate the sludge in a more variable environment, including interactions with rainfall. The two experimental conditions were: saturated with a constant water cap of approximately 10 cm of rainwater, and unsaturated creating periods of wetting and drying due to rainfall. Both conditions were designed to allow rainfall to flow through the sludge into a collection container. A schematic of the set up (Figure 3.1) shows the placement of the collection containers, strategically placed with tubing to maintain a constant water level for the saturated column. These weathering experiments were constructed on the mine site in New Zealand, with monthly water sampling of the collection buckets for 22 months. After one year solid samples were collected for geochemical phase extractions, and microsensor measurements were taken on site.

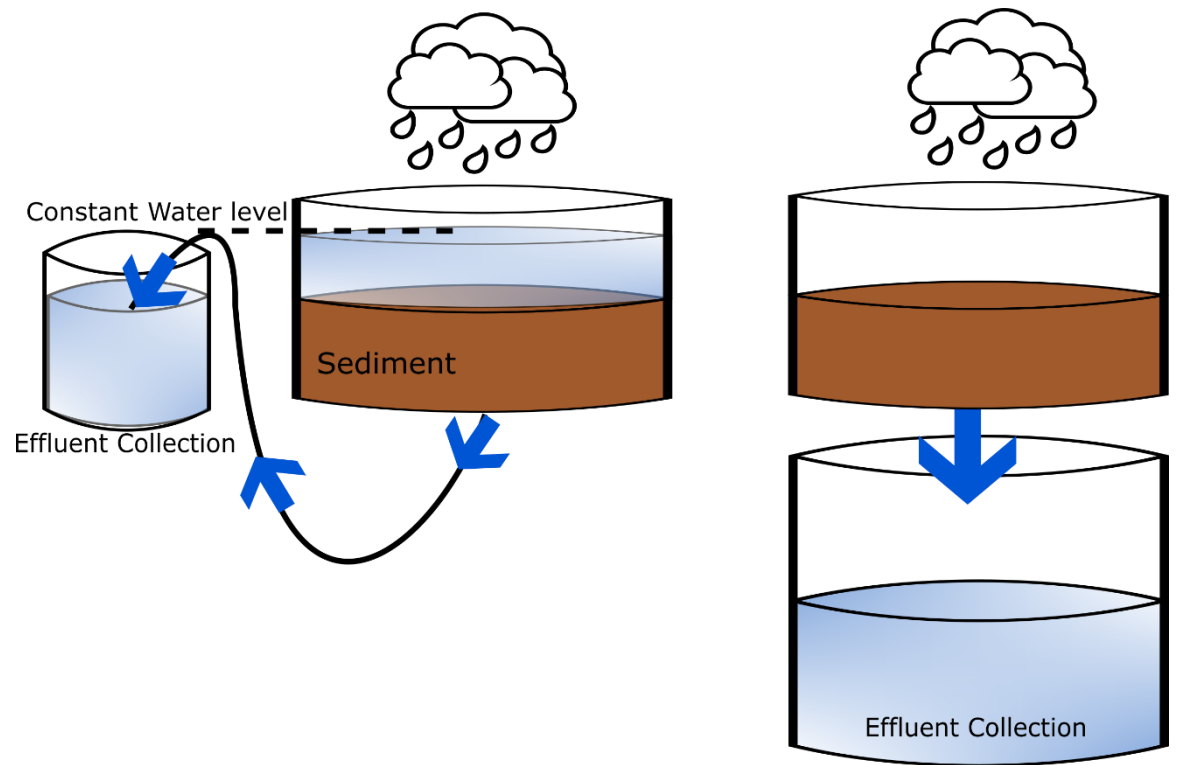


**Figure 3.1** Schematic of field experiment showing the saturated (left) and unsaturated (right) flow through columns and collection containers.

### 3.2.2 Micro sensors and diffusive flux calculations

#### *Micro-sensor profiles*

HS<sup>-</sup>, O<sub>2</sub>, and redox microelectrode sensors (Unisense Science, Denmark) were used to measure vertical gradients across the sediment water interface. In this case, around 2 cm directly above and below the sediment water interface was analysed in order to calculate the slopes of the concentration gradient, a method developed by Revsbech, (1989) although methods by Reid et al. (2016) were more specifically followed for collection. Sensors were controlled via a computer fitted with SensorTrace Pro software and the Unisense Microsensor Multimeter. The microsensors had 10 µm (H<sub>2</sub>S) and 500µm (Oxygen) glass tips and were fitted to a manual micro manipulator that allowed measurements to be taken at precise depths every 0.5mm, at least 1 cm above the sediment water interface. For each point, three measurements were recorded, and the profile used the average. Calibration and pre-polarization guidelines were followed from the Unisense prescribed procedures. The profile was taken after one year in the field.

#### *Diffusivity measurement and flux calculations*

A diffusivity sensor (50 µm) was used to measure diffusivity constants in all microcosms at the end of the incubation period. This required a two point calibration (Revsbech et al. 1998) and an inert gas, which in this case was 5% H<sub>2</sub> mixed with 95% N to calculate flux of O<sub>2</sub> and HS<sup>-</sup>. Due to the need of gas flow, the diffusivity constant could not be measured in the field, so measurements recorded in the lab were used. A slope calculated from the profiles of O<sub>2</sub> and HS<sup>-</sup> was used with the diffusivity measurement in the following equation:



$$J(x) = -\emptyset D(x) \frac{dC(x)}{dx} \quad [\text{cm}^2\text{S}^{-1}] \quad \text{Eq. 2}$$

$J(x)$  is flux;  $-\emptyset D(x)$  is the diffusivity measured using the diffusivity sensor on the sediment; and  $dC(x)/dx$  is the slope of the  $\text{HS}^-$  and  $\text{O}_2$  concentration profile measured along the sediment-water interface.

### 3.2.3 Metal analysis from flow through

The water in the effluent collection containers was measured monthly for pH using a field probe on site. At the sample time water samples were preserved, and later analyzed for metals. Dissolved concentrations of Al, Ca, Fe, Ni, and Zn were conducted using ICP-MS, APHA 3125 B 22<sup>nd</sup> ed., and sulphate using ion chromatography, APHA 4110 B 22<sup>nd</sup> ed., (Hill Laboratories, New Zealand). Using the concentrations of the effluent of the columns, the volume of sludge used, and the recorded volume of water that flowed through the system, an estimate based on the mg of metal per kg of material that has the possibility to be released was made. In order to determine the correlation between rainfall and metal concentration, a Pearson correlation test was done in PAST, to determine the magnitude and the significance of the correlation.

### 3.2.4 Geochemical phase descriptions

Geochemical phase analyses were performed using the same methods as Chapter 2 (Butler et al. 2019) section 2.2.3. Five phases were analysed including water-soluble; bio-available (EDTA); amorphous oxyhydroxide phases (reducible); strong acid extractable; and metals weakly bonded to oxide phases (weak acid) found in table 2.1 (chapter 2). Metals on the extractant fluid was analyzed using 700 series Agilent 720-ES ICP-OES system. PCA was done using PAST to determine the effects of having a water cap

compared to the unsaturated environments. Both saturated and unsaturated columns were compared to the initial sediment (also used in Chapter 2) to determine the amount of metals that had leached out from the sludge due to rainwater flow through.

### **3.2.5 Hydrological predictions**

To predict the lifespan of the MSB, the following assumptions were made: (1) the only source of Ca flowing out of the MSB is from the mussel shells; (2) Ca is not reprecipitating somewhere else within the reactor; and (3) the concentration of Ca in the inflow and outflow is relatively constant as an average concentration was used. With these assumptions, the lifespan of the bioreactor was calculated using a mass balance. With an estimation of the total amount of Ca in the MSB, and monthly measurements of the outflow and the inflow an estimate of the amount of Ca was made. Monthly measurements of Ca from the effluent and effluent of the reactor was made using ICP-MS, APHA 3125 B 22<sup>nd</sup> ed by hill laboratories in New Zealand. The flow rates from 2012 to 2015 were previously calculated (Diloreto 2016), and were updated to 2017 for this purpose. To estimate the volume of water which the MSB treats, an omnilog WT-HR water level logger by Intech Instruments was placed within the MSB. The omni-log measures the water level on top of the MSB which can be modeled to predict the rate of flow and total amount of water passed through. Using the Ca volumes and flow rates, the rate at which the shells are being dissolved, can be approximated. Using the approximated rate, a lifespan of the MSB can be predicted based on the dissolution of the calcium carbonate.

### 3.3 Results and discussion

#### 3.3.1 Chemical profiles and flux

Oxygen and H<sub>2</sub>S concentrations were measured *in situ* after 1 year of weathering and leaching by rainfall. Oxygen decreased to zero 1 cm below the sediment water interface and fluctuated between 4.5 to 6.5 mg/l in the water column (Figure 3.2). This fluctuation may have been caused by biofilm and algae growing above the sediment (Figure 3.3). When the oxygen concentrations were low, there was also a peak of H<sub>2</sub>S at 20 µmol/L at around 0.75cm, which would suggest the reduction of sulfate, and the presence of SRB. Flux was calculated using the oxygen profile in figure 3.2 and the diffusivity constant was measured in the laboratory for the oxic biological active incubation, as this would be most similar to the field mesocosm. Flux was calculated to be 2.66 mmol m<sup>-2</sup> day<sup>-1</sup>, which was comparable to flux values calculated for the laboratory incubations. There were notable similarities between the laboratory (Butler et al. 2019) and the field even though the field study was a more dynamic environment. The flux of the oxygen and hydrogen sulfide are comparable to the laboratory study. Hydrogen sulphide was measured in the sludge at more than double the concentrations measured in the anoxic laboratory incubation, suggesting a possible active population of sulfate reducing bacteria (SRB). Though no microbial community analysis was done on the field samples, the presence of hydrogen sulphide is an indicator of SRB, that required a source of organic carbon (Logan et al. 2003). Due to the more dynamic environment, and deposition of organic matter (algae visible- Figure 3.3), the SRB community may have been more active in the anoxic zone of the field study than in the lab incubation. The lab study showed that there is the potential for SRB to be sourced from the oxic sludge and

thrive in the organic rich anoxic depths of the sludge, especially under a water cap. If SRB were present in the field study, they could increase the stability of the sludge under certain conditions as they would immobilize some metals.

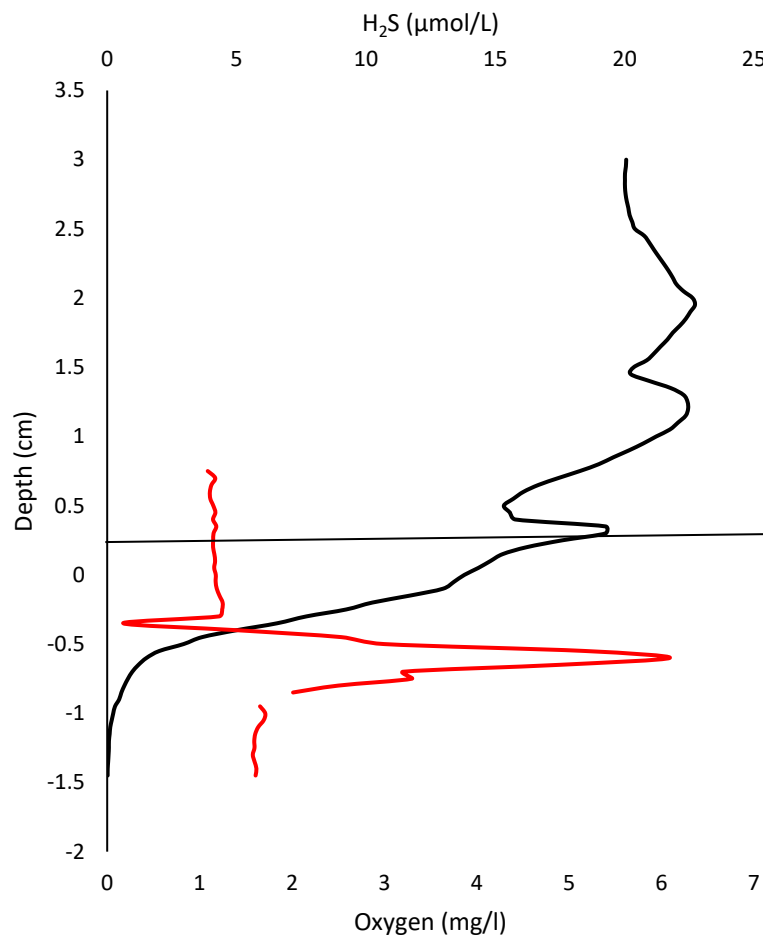


**Figure 3.2** Oxygen (black) and hydrogen sulfide (red) concentration profiles, in mg/l (oxygen) and  $\mu\text{mol/L}$  (hydrogen sulfide) collected from the saturated field column after one year.



**Figure 3.3** Leaching columns after one year, showing the saturated (top) and unsaturated (bottom).

### 3.3.2 Time series

Metals released from the field mesocosms were variable based on monthly samples, assumingly due to weather and seasonal changes. The pH of the water flowing through the sediment did appear to be associated with rainfall, with high amounts of rain producing a higher pH, up to 6 (Figure 3.4). For the unsaturated (dry) experiment, some variance can be significantly ( $p\text{-value}=0.02$ ) correlated with rainfall based on a pearson correlation ( $r=0.49$ ). The saturated did not have a significant correlation ( $p\text{-value}=0.08$ ) with ( $r=0.39$ ). As rainfall in New Zealand typically ranges between a pH 5 and 6 (New Zealand Government 1997), the sludge appeared to have produced some acidity, especially in months with low rainfall, when the pH was measured at 3.75. The capability of the sediment to produce acidity did not seem to decrease with time. The saturated mesocosm pH did not have a correlation with the amount of rainfall and resulted in an overall lower pH with a general decrease in pH over time. This is most likely a result of the time that the water had to interact with the sediment, as in the saturated mesocosm the rainwater had a longer time to interact with the sediment and produce a lower pH.

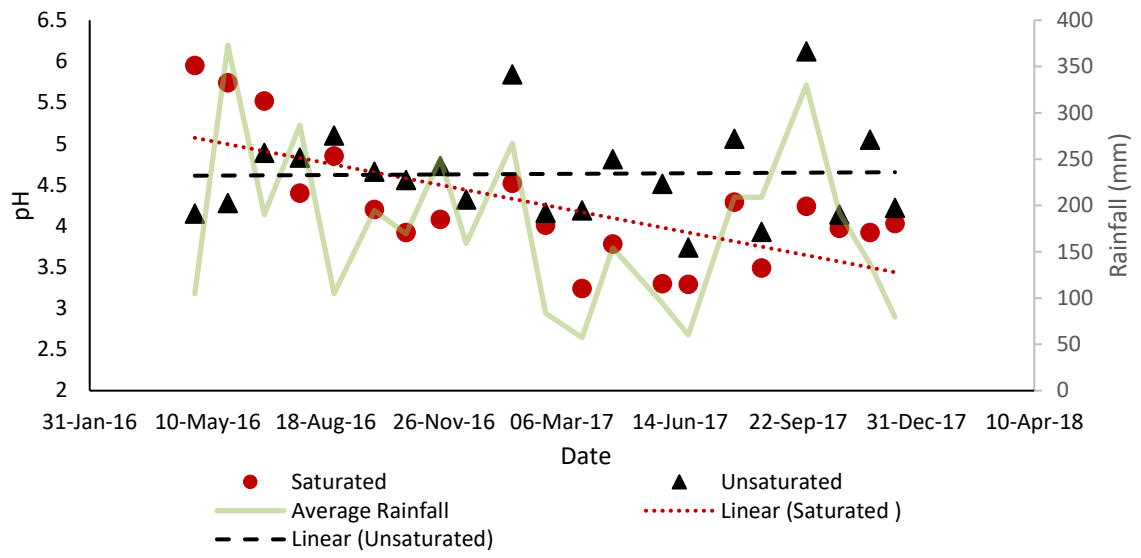


**Figure 3.4** pH of the effluent water measured monthly on site, compared to the averagely monthly rainfall in mm near the mine site.



Sulfate concentrations are a product of AMD (Evangelou and Zhang 1995; Akcil and Koldas 2006; Schippers et al. 2010a) and were initially over 120 mg/L for the unsaturated mesocosm but fluctuated at around 40 mg/L for the rest of the time studied (Figure 3.5). Seeps within the mine have been measured to be 172.6 mg/L (DiLoreto et al. 2016a) so the concentration is relatively low compared to the AMD site. The sludge was sourced from an oxic environment and most sulfides would have already been oxidised. Sulfate in the system could have also been reduced by SRB that would have been present below the sediment water-interface where oxygen concentrations were quite low and  $\text{H}_2\text{S}^-$  gas was measured. Small amounts of Fe ( $< 3$  mg/L) for both mesocosms were found in the drainage water and the concentrations do not seem to vary based on the average daily rainfall (Figure 3.5). Concentrations for the unsaturated mesocosm were mostly below detection limits, apart from the end of the time series. Zinc concentrations were higher in the unsaturated mesocosm in the early part of the time series, while the saturated concentrations were higher at the end of the time series. For most of the months in the unsaturated mesocosm, the concentrations were above the recommended concentration of Zn for the survival of 80% of the species in freshwater (0.03 mg/L), and almost all months were higher than the 95% survival rate (0.008mg/L) (CCME 1999). Using the monthly metal concentrations measured and the total amount of water collected as an average of metals released from the sludge in that month, contaminants released per kg of sludge were calculated (table 3.1). These rates suggest that more Al, Ni, and Zn would be released in an unsaturated environment, and higher concentrations of Fe would be released in the saturated. In order to determine which geochemical phase these metals were leaching, the geochemical phases were analysed and compared to the initial sludge.

**Table 3.1** Metals (mg) released per kg of sludge in one month, calculated from a average over a 22 month period.

	Aluminium	Calcium	Iron	Nickel	Zinc
Saturated	0.70	13.68	1.75	0.03	0.06
Unsaturated	2.59	36.54	0.08	0.04	0.12

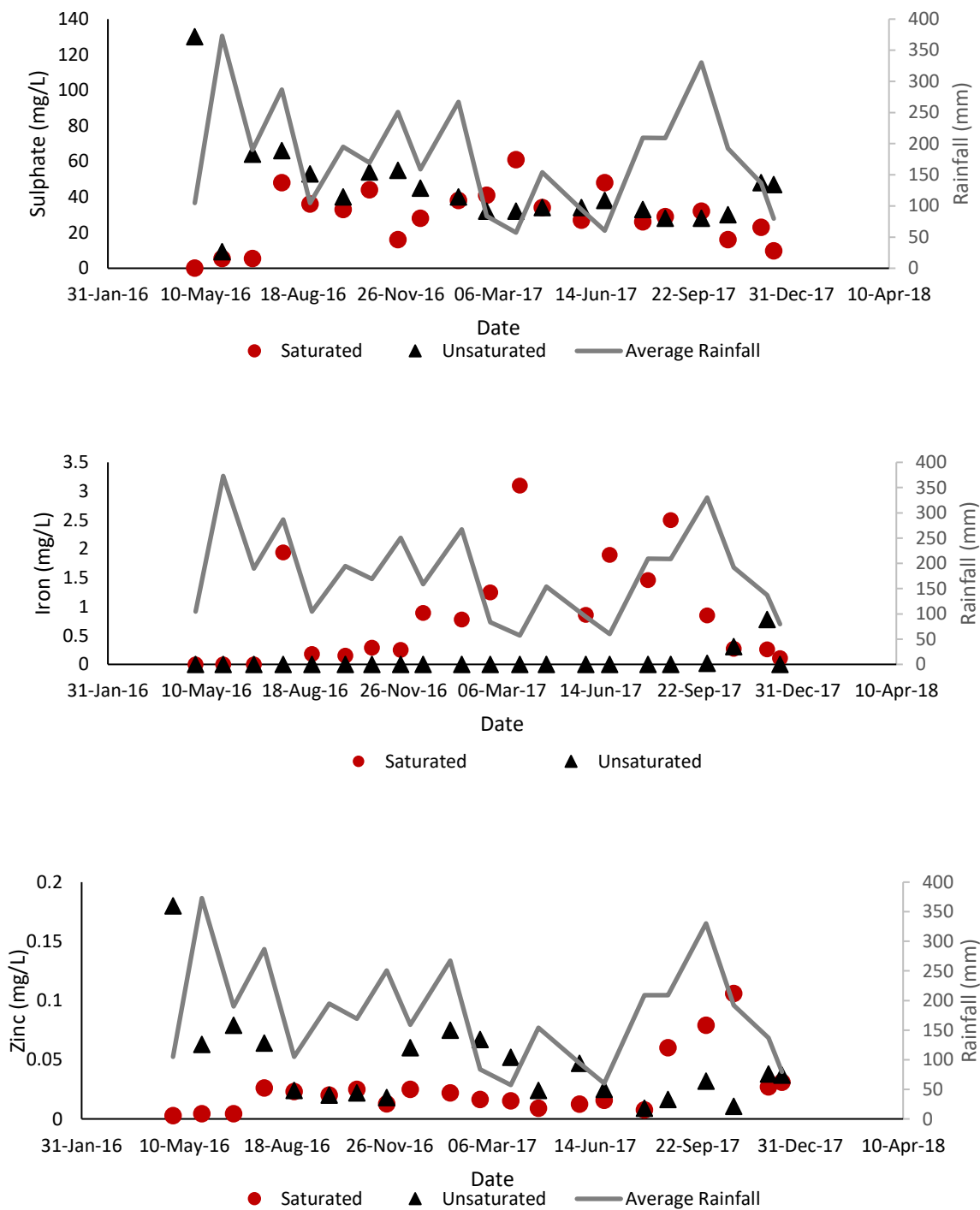


**Figure 3.5** Time series for sulfate, iron, and zinc in mg/l for both the saturated and unsaturated columns, compared to the average rainfall for the area.

### 3.3.3 Geochemical phase descriptions

Geochemical phases were analyzed using selective extractions after 12 months for both field mesocosms in order to understand the long-term effects of the sediment in a natural environment and interactions with rainwater *in situ*. Table 3.2 depicts metals within each geochemical phase, as well as statistical differences between field environments, noted by gray shading. Comparing the initial (time 0) to the column experiment determined the concentration of metals that were lost due to leaching from rainfall. A PCA analysis was used to compare the two conditions and the initial (appendix Figure A6-7). The three sample groups within the amorphous hydroxides, weakly bound to iron oxides, and strong acid all had some overlap, while the water soluble and organically bound sample groups all plotting in separate quadrants. The variance within the strong acid extractable was explained by PC1 (64%) and PC2 (23%), with strong loadings of Fe (0.9). Iron concentrations in the sludge were initially  $9500 \pm 1000$  mg/kg and up to 1000 mg/kg may have been lost in the saturated column. The strong acid extraction determined the total extractable metals and there were no significant changes in metals of interest after one year of leaching. However, other phase extractions did detect changes between the initial and final samples, suggesting that total extractable metals were not sensitive enough to detect smaller changes in concentrations. The PCA suggested that the organically bound and water-soluble phases were affected by the weathering conditions. The variance of the organically bound phase is controlled by PC1 (70%) and PC2 (26%), which have strong loadings of Ca (0.9) and sulfur (0.3). Zn, Al, Ca, Fe, Mn, S, had a significant decrease (over 10x) after the leaching experiments. These metals would have been dissolved by rainwater in both experimental conditions, and it suggests that the metals associated with organic phases are not stable with in dry or

saturated environments. The water-soluble phase also showed significant changes based on the PCA and 96% of the variance was controlled by PC1. There were some differences in the two experimental conditions in the water-soluble phase as Mn, Zn, and Al concentrations were higher in the saturated experiment, suggesting that the water-soluble phase was more stable in this condition as the metals were not removed from the sludge by rainwater. The unsaturated mesocosm generally had lower concentrations of metals in water-soluble fractions than the initial, which suggested water-soluble metals would be less stable in a dry, unsaturated environment such as the mine surface. Organically bound metals all decreased after weathering experiments, suggesting that this phase was not stable after 12 months of interaction with rainwater. Significant changes were not found for the amorphous hydroxides, or weakly bound to iron oxide phase, indicating that these phases, are somewhat stable in either saturated or unsaturated environments.

The phase data from both the laboratory and field data describe the labile metal concentrations, describing risks of Zn concentrations associated with oxide mineral phases and low concentrations in the water-soluble phases. Zn concentrations released from the field mesocosm were high compared to the recommended values for aquatic life. For the unsaturated environments, Zn appears to have been leached from the water-soluble portions of the sludge, suggesting that storing the sediment on a mine surface may cause high levels of Zn to be released. In the saturated environment, the most significant change in Zn concentrations were within the organically bound portion, suggesting that bioavailable Zn was the most labile fraction of Zn when stored in saturated sediment with a water-cap. Based on the time series of Zn concentration in the effluent of the sludge, this only occurred during the end of the 22 months suggesting Zn became more labile

with time. In the saturated leaching column, the Zn concentrations of the water-soluble phase was higher than in the unsaturated, though these were analysed at 12 months, so the higher concentrations in the effluent after 20+ months could be due to the labile Zn eventually leaching out. The Zn could be leaching out of the labile phases in the saturated column due to the increase in pH by the end of the experiment (Figure 3.4). By June 2017 the pH of the flow through saturated experiment is around 3.5 to 4, which could cause the more labile Zn to be leached out.

With the exception of Fe, more metals were released in the unsaturated column overall. An unsaturated environment is more prone to having cracks form in the dried sediment, and this means that oxygen will most likely penetrate deeper into the sludge, increasing dissolution rates, which was observed in other sludge weathering studies (Demers et al. 2017). More Zn and Al were released per kg of material in the unsaturated sludge, and more Fe was released in the saturated.

**Table 3.2** Chemical phase extractions for the final shaded cells identify which samples are significantly different based on a t-test.

Metal mg/kg		Al	Ca	Fe	Mg	Mn	S	Zn
Chemical Phase								
Water	Saturated	19 ± 6	180 ± 40	<DL	18 ± 3	36 ± 7	143 ± 8	0.3 ± 0.1
	Unsaturated	1.5 ± 1.5	210 ± 70	<DL	10 ± 8	0.4 ± 0.1	130 ± 50	0.08 ± 0.04
	Initial	1.6 ± 0.5	360 ± 90	<DL	32 ± 5	60.0 ± 10	260 ± 50	0.5 ± 0.2
Bioavailable	Saturated	12 ± 3	20 ± 2	11 ± 4	4.1 ± 0.2	1.8 ± 0.3	19 ± 3	0.07 ± 0.01
	Unsaturated	16 ± 2	30 ± 5	5 ± 1	4.3 ± 0.2	3.0 ± 1	20 ± 2	0.2 ± 0.1
	Initial	460 ± 4	300 ± 20	210 ± 60	6.0 ± 0.7	70.0 ± 10	360 ± 30	1.0 ± 0.4
Reducing	Saturated	620 ± 90	560 ± 160	1500 ± 200	140 ± 40	66.5 ± 60	780 ± 100	1.8 ± 0.3
	Unsaturated	670 ± 150	670 ± 240	1400 ± 300	140 ± 30	98.3 ± 40	830 ± 70	3.3 ± 0.7
	Initial	350 ± 60	880 ± 100	1200 ± 300	160 ± 10	70.0 ± 10	780 ± 70	2.0 ± 0.3
weak acid	Saturated	1100 ± 160	830 ± 100	2825 ± 374	270 ± 20	66 ± 5	700 ± 300	9 ± 3
	Unsaturated	1200 ± 130	1100 ± 200	2481 ± 779	260 ± 60	130 ± 20	1000 ± 100	22 ± 7
	Initial	1200 ± 200	1200 ± 200	2600 ± 300	280 ± 40	150 ± 40	600 ± 60	10 ± 5
strong acid	Saturated	1400 ± 120	680 ± 85	8300 ± 530	1280 ± 50	100 ± 20	1000 ± 300	30 ± 7
	Unsaturated	1400 ± 190	900 ± 100	9000 ± 1100	1480 ± 120	190 ± 50	1700 ± 400	50 ± 8
	Initial	1300 ± 200	800 ± 100	9500 ± 1000	1700 ± 200	160 ± 30	800 ± 60	30 ± 5

### 3.3.4 Lifespan predictions based on mass balance of calcium

The MSB contains around 362 tons of mussel shells, which are 88-95wt%  $\text{CaCO}_3$ . The other 5-12wt% was composed of organic material. As a result, the total amount of calcium in the system was between 128 000 and 136 000 kg. Using the concentrations of Ca in both the inflow and outflow of the system, a mass balance was completed to determine how long the reactor could theoretically last. The total amount of water passed through the reactor was estimated to be 200 000  $\text{m}^3$  up to the end of 2016. Around 17 000 kg of Ca (42 000 kg of  $\text{CaCO}_3$ ) over 4 years was removed from the reactor based on the outflow-inflow monthly concentration (Figure 3.5). This indicates that between 86 and 88.5% of the reactor is unreacted mussel shells. This translates to a lifespan prediction of 29-31 years. The amount of water that could have passed through the reactor if the sludge was not impeding flow was calculated based on constant flow rates measured initially in the reactor at around 500 000  $\text{m}^3$ . This number was used to calculate the length of time the reactor would theoretically last, if the sludge was not an issue, shown to be 12-13 years.

Having the sludge layer impeding the flow of AMD led to unreacted mussel shells in the bottom of the reactor, as large amounts of AMD were not able to reach them. Once removed in Feb 2016, the flow rates did not have a large increase as originally expected (Figure 3.6). If the flow continues at the same rate, the reactor is expected to last another 29-31 years; however, if the hydrological issues are not fixed, the MSB flow may stop completely. The MSB would most likely be better placed in a site with very low sedimentation rates, rather than an active site. There is also a possibility of installing some sort of barrier system to decrease the amount of sediment inputs deposited into the system.



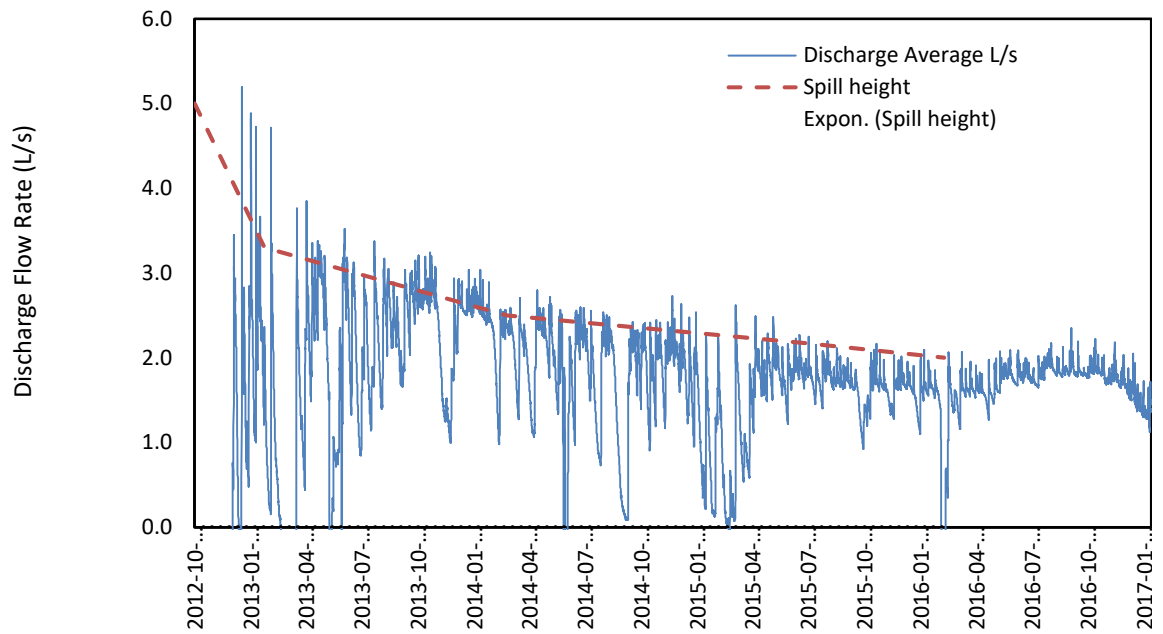


**Figure 3.6** An updated figure from DiLoreto et al., (2016a) showing flow rates from 2012 to 2017.

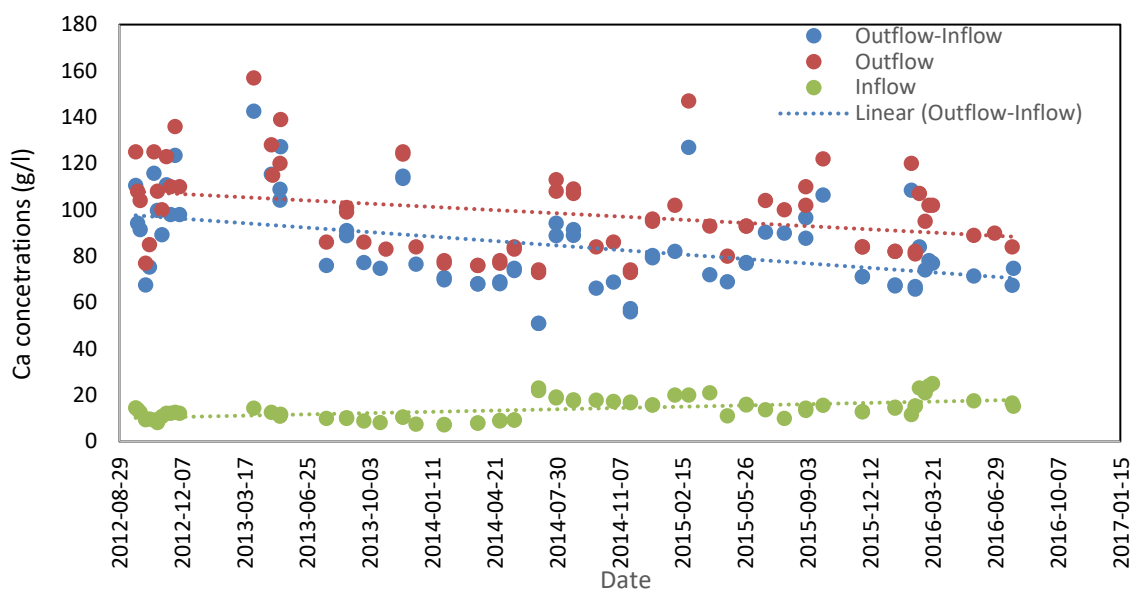


**Figure 3.7** Calcium concentrations of the inflow and outflow from the MSB, as well as the outflow-inflow which describes the amount of calcium dissolved from the mussel shells.

### 3.4 Conclusions

Based on the laboratory study (Chapter 2) the sludge could potentially be stored in any anoxic zone, such as the bottom of a tailings pond or acting as an oxygen barrier for other mine wastes. This field study determined the effects of saturated and unsaturated environments with influence of rainfall potential for metals to be leaching out of the sludge. Under dry conditions, there was a greater risk of more labile metals (such as Zn) being remobilized. Overall, more metals were leached over a 22 month period in the unsaturated column than in the saturated, most likely coming from water soluble and organically bound phases, as these had high decreases from the initial geochemical phases. There is still a potential of some metals being remobilized in a saturated environment (Fe), and the pH was lower which still suggests some risks. Compared to the laboratory study, the field columns had similar flux values for both oxygen and H<sub>2</sub>S. This confirms that the laboratory incubations were successful in representing a field environment, though reactions occurring in the field may have been elevated due to increased sources of organic material, and constant flow of rainfall. MSB are an effective way to treat AMD, however the low permeability sludge must be stored effectively, and this study based on field leaching columns, suggested that this is in a saturated environment.

### 3.5 References

- Akcil A, Koldas S (2006) Acid Mine Drainage (AMD): causes, treatment and case studies. *J Clean Prod* 14:1139–1145. doi: 10.1016/j.jclepro.2004.09.006
- Butler S, Pope J, Chaganti S, et al (2019) Biogeochemical Characterization of Metal Behavior from Novel Mussel Shell Bioreactor Sludge Residues. *Geosciences* 9:50. doi: 10.3390/geosciences9010050
- Chao A (1984) Nonparametric Estimation of the Number of Classes in a Population. *Scand. J. Stat.* 11:265–270.
- Chen M, Walshe G, Chi Fru E, et al (2013) Microcosm assessment of the biogeochemical development of sulfur and oxygen in oil sands fluid fine tailings. *Appl Geochemistry* 37:1–11. doi: 10.1016/J.APGEOCHEM.2013.06.007
- Clark DA, Norris PR (1996) *Acidimicrobium ferrooxidans* gen. nov., sp. nov.: mixed-culture ferrous iron oxidation with *Sulfobacillus* species. *Microbiology* 142:785–790. doi: 10.1099/00221287-142-4-785
- Demers I, Benzaazoua M, Mbonimpa M, et al (2015) Valorisation of acid mine drainage treatment sludge as remediation component to control acid generation from mine wastes, part 1: Material characterization and laboratory kinetic testing. *Miner Eng* 76:109–116. doi: 10.1016/j.mineng.2014.10.015
- Demers I, Mbonimpa M, Benzaazoua M, et al (2017) Use of acid mine drainage treatment sludge by combination with a natural soil as an oxygen barrier cover for mine waste reclamation: Laboratory column tests and intermediate scale field tests. *Miner Eng* 107:43–52. doi: 10.1016/j.mineng.2016.11.017
- DiLoreto ZA, Weber PA, Olds W, et al (2016a) Novel cost effective full scale mussel shell bioreactors for metal removal and acid neutralization. *J Environ Manage.* doi: 10.1016/j.jenvman.2016.09.023
- DiLoreto ZA, Weber PA, Weisener CG (2016b) Solid phase characterization and metal deportment in a mussel shell bioreactor for the treatment of AMD, Stockton Coal Mine, New Zealand. *Appl Geochemistry* 67:133–143. doi: 10.1016/j.apgeochem.2016.02.011
- Edgar RC (2010) Search and clustering orders of magnitude faster than BLAST. *Bioinformatics* 26:2460–2461. doi: 10.1093/bioinformatics/btq461
- Edgar RC, Haas BJ, Clemente JC, et al (2011) UCHIME improves sensitivity and speed of chimera detection. *Bioinformatics* 27:2194–2200. doi: 10.1093/bioinformatics/btr381
- Falk N, Chaganti SR, Weisener CG (2018) Evaluating the microbial community and gene regulation involved in crystallization kinetics of ZnS formation in reduced

- environments. *Geochim Cosmochim Acta* 220:201–216. doi: 10.1016/J.GCA.2017.09.039
- Fangueiro D, Bermond A, Santos E, et al (2002) Heavy metal mobility assessment in sediments based on a kinetic approach of the EDTA extraction: Search for optimal experimental conditions. *Anal Chim Acta* 459:245–256. doi: 10.1016/S0003-2670(02)00134-4
- Ferris FG, Tazaki K, Fyfe WS (1989) Iron oxides in acid mine drainage environments and their association with bacteria. *Chem Geol* 74:321–330. doi: 10.1016/0009-2541(89)90041-7
- Florentino AP, Weijma J, Stams AJM, Sánchez-Andrea I (2015) Sulfur Reduction in Acid Rock Drainage Environments. *Environ Sci Technol*. doi: 10.1021/acs.est.5b03346
- Frankel RB (2003) Biologically Induced Mineralization by Bacteria. *Rev Mineral Geochemistry* 54:95–114. doi: 10.2113/0540095
- Gadd GM (2010) Metals, minerals and microbes: Geomicrobiology and bioremediation. *Microbiology* 156:609–643. doi: 10.1099/mic.0.037143-0
- CCME (1999) Canadian Water Quality Guidelines for the Protection of Aquatic Life INTRODUCTION.
- Demers I, Mbonimpa M, Benzaazoua M, et al (2017) Use of acid mine drainage treatment sludge by combination with a natural soil as an oxygen barrier cover for mine waste reclamation: Laboratory column tests and intermediate scale field tests. *Miner Eng* 107:43–52. doi: 10.1016/j.mineng.2016.11.017
- Diloreto ZA (2016) Scholarship at UWindsor Biogeochemical Investigations of a Full Scale Mussel Shell Bioreactor for the Treatment of Acid Mine Drainage ( AMD ), the Stockton Mine , New Zealand.
- DiLoreto ZA, Weber PA, Olds W, et al (2016a) Novel cost effective full scale mussel shell bioreactors for metal removal and acid neutralization. *J Environ Manage*. doi: 10.1016/j.jenvman.2016.09.023
- DiLoreto ZA, Weber PA, Weisener CG (2016b) Solid phase characterization and metal deportment in a mussel shell bioreactor for the treatment of AMD, Stockton Coal Mine, New Zealand. *Appl Geochemistry* 67:133–143. doi: 10.1016/j.apgeochem.2016.02.011
- Evangelou VP (Bill), Zhang YL (1995) A review: Pyrite oxidation mechanisms and acid mine drainage prevention. *Crit Rev Environ Sci Technol* 25:141–199. doi: 10.1080/10643389509388477

- Logan M, Ahmann D, Figueroa L (2003) Assessment of Microbial Activity in Anaerobic Columns Treating Synthetic Mine Drainage 1. *Jt Conf 9th Billings L Reclam Symp 20th Annu Meet Am Soc Min Reclam June 3-6, 2003* 0658. doi: 10.21000/JASMR03010658
- McCauley C, O'Sullivan A, Weber P, Trumm D (2010) Variability of Stockton Coal Mine drainage chemistry and its treatment potential with biogeochemical reactors. *New Zeal J Geol Geophys* 53:211–226. doi: 10.1080/00288306.2010.503565
- McCauley CA, O'Sullivan AD, Milke MW, et al (2009) Sulfate and metal removal in bioreactors treating acid mine drainage dominated with iron and aluminum. *Water Res* 43:961–970. doi: 10.1016/j.watres.2008.11.029
- New Zealand Government (1997) The State of New Zealand's Air | Ministry for the Environment. <http://www.mfe.govt.nz/publications/environmental-reporting/state-new-zealand's-environment-1997-chapter-six-state-our-ai-6>. Accessed 15 Sep 2018
- Pope J, Weber P, Mackenzie A, et al (2010) Correlation of acid base accounting characteristics with the Geology of commonly mined coal measures , West Coast and Southland , New Zealand. doi: 10.1080/00288306.2010.498404
- Reid T, Boudens R, Ciborowski JJH, Weisener CG (2016) Physicochemical gradients, diffusive flux, and sediment oxygen demand within oil sands tailings materials from Alberta, Canada. *Appl Geochemistry* 75:90–99. doi: 10.1016/J.APGEOCHEM.2016.10.004
- Revsbech NP (1989) Diffusion characteristics of microbial communities determined by use of oxygen microsensors. *J Microbiol Methods* 9:111–122. doi: 10.1016/0167-7012(89)90061-4
- Revsbech NP, Nielsen LP, Ramsing NB (1998) A novel microsensor for determination of apparent diffusivity in sediments. *Limnol Oceanogr* 43:986–992. doi: 10.4319/lo.1998.43.5.0986
- Schippers A, Breuker A, Blazejak A, et al (2010) The biogeochemistry and microbiology of sulfidic mine waste and bioleaching dumps and heaps, and novel Fe(II)-oxidizing bacteria. *Hydrometallurgy* 104:342–350. doi: 10.1016/J.HYDROMET.2010.01.012
- Trumm D, Ball J, Pope J, Weisener C (2015) Passive Treatment of ARD Using Mussel Shells – Part III : Technology Improvement and Future Direction. *10th Int Conference Acid Rock Drain IMWA Conf* 1–9.
- Uster B, O'Sullivan AD, Ko SY, et al (2014) The Use of Mussel Shells in Upward-Flow Sulfate-Reducing Bioreactors Treating Acid Mine Drainage. *Mine Water Environ* 34:442–454. doi: 10.1007/s10230-014-0289-1

Weisener C, Weber P (2010) Preferential oxidation of pyrite as a function of morphology and relict texture. *New Zeal J Geol Geophys* 53:167–176. doi: 10.1080/00288306.2010.499158

## **Chapter 4**

### **Conclusions and Future Work**

#### **4.1 Conclusions and implications**

This thesis addressed concerns involving potential storage of sludge in both laboratory and field studies. MSB is both an efficient and cost effective method to treat AMD (McCauley et al. 2009b; Uster et al. 2014; Trumm et al. 2015; DiLoreto et al. 2016a). However, if concerns about the sludge layer are not addressed, the effective life span of the reactor drastically decreases to approximately 5 years, compared to the theoretical lifespan based on calcium carbonate dissolution (29-31 years). The sludge layer was removed to solve the problems with flow, however the sludge then requires storage or utilization in some way on the mine site. This study was designed to provide information on management practices that reduce the risk of metal contamination.

The study question led to a testable hypothesis that an oxic storage environment would increase the risk of contamination. This was thought to be a result of the increased metal oxides that would be produced, and the chemically sorbed species associated with them. This hypothesis held true for the geochemical phase data as there were higher concentration of Fe associated with oxyhydroxides, higher Zn sorbed to oxides, and higher labile Mn, Al, and S all in the oxide phases all potential risk factors. The hypothesis also predicted that risk factors of contamination would increase due to microbial activity, specifically iron oxidizers. The design of the mesocosms allowed this to be tested as there was abiotic and biotic conditions. The results concluded that only the



oxyhydroxide phase was significantly affected by microbiology, providing t partial support of the hypothesis. A second part of the hypothesis predicted that an abundance of iron oxidizing bacteria would be found and would therefore be most likely responsible for this increase. However, due to sequencing limitations (primer specificity and sequencing platform) this study was not able to confirm the presence of known iron oxidizers in these mesocosms to a species level (e.g *acidimicrobium ferrooxidans*). Though there were sequences identified at higher taxonomic classifications of that species such as the family (*Acidobacteriaceae*) or order (*Acidimicrobiales*), these are potential iron oxidizers and would likely have been responsible for the increase in iron associated with oxyhydroxides.

In comparison the anoxic mesocosm was hypothesized to have fewer risks associated with metal contamination. This hypothesis held true as most metals associated with labile phases were at higher concentrations in the oxic mesocosm. It was thought that this would have been due to the presence of SRB and the subsequent increased sulfide formation which would sequester metals. This hypothesis held true, as genera of SRB were identified as significantly differentially abundant in the anoxic incubations compared to the oxic. They were most likely responsible for increased sulfide particles in the biotic oxic system. This finding is significant, as the sludge was sourced from a oxic environment, where SRB would not be very active. The SRB could have been living in pockets of anoxia in the oxic sludge, and once placed into the anoxic environment, they were able to populate quickly.

In chapter three the sludge was studied under dynamic environmental conditions, testing both saturated and unsaturated storage environments. It was hypothesized that rainwater would cause increased metal dissolution in the unsaturated environment. The results found that the unsaturated column appeared to be more correlated to rainfall (based on pH) and that there was a greater risk of more labile metals (such as Zn) being remobilized especially in the beginning of the experiment. The unsaturated column had more labile metals leaching out much quicker. In the saturated column the pH was not significantly correlated to rainfall and it appeared to steadily decrease. This could have caused an increase of metal leaching (such as Zn) towards the end of the experiment. The saturated column also had higher concentrations of Fe compared to the unsaturated, but the concentrations were relatively low. By Comparison more metals were shown to leach out over the 22 month period for the unsaturated column. Based on this observation it suggests that this may be the best option for increasing the stability of the sludge.

Mussel shells are a cheap and effective substrate that can be used in AMD remediation. Based on the results of this study, If a sludge slayer has built up, and is then removed, the best storage option would be an anoxic saturated environment. It may also have the possibility to be utilized as an oxygen barrier for the storage of mine tailings or waste rock.

## **4.2 Future work**

Further microbial assessment should be done to increase the depth of taxa representation and to further assess and quantify the relative gene expression through RT qPCR. Additionally, while taxonomic information can be useful, it would be

advantageous to perform a metatranscriptomic study or a comparison with cDNA analysis. Such methods provide data for only the active community of microbes, while the rDNA 16s meta-barcoding may inadvertently provide information on dead microbes as well as active. Further microbial studies would also be useful on the entirety of the MSB, as well as studies on the sludge characterization. In order for both quantitative real-time PCR and metatranscriptomic analyses to occur there must be successful extraction of RNA. This is difficult as the AMD contains many inhibitors and conditions which degrade or bind RNA, such as low pH and clay particles (Novinscak and Fillion 2011). Few studies have successfully extracted RNA from AMD and those that have, typically extracted RNA from filtered water, and not from the actual sediment (Kuang et al. 2013; Chen et al. 2014). Analysis of the sediment would be more valuable in studies investigating biogeochemical connections, as it would provide a way to have a direct comparison to the geochemistry within sediment and on the sediment water interface rather than just within the water column. Optimization of extraction methods would be required to determine the most effective RNA extraction procedure, which will most likely involve extra buffering and purification steps.

Further studies could be done to test different management practices in the field such as use within soil blends or as an oxygen barrier with tailings or waste rock. Field leaching columns could be designed much like Chapter 3, using different soil to sludge ratios, or testing the sludges ability to act as an oxygen barrier. These leaching experiments could help the mining company make decisions for sludge management and utilization rather than just storage of the sludge as addressed in this study. The sludge layer was removed

to increase the permeability of the MSB. Based on data presented in Chapter Three, sludge was not the only factor impeding flow. There were also problems with sediment being deposited within pore spaces of the mussel shells, as well as the mussel shells possibly naturally compressing over time. Based on the first few months after removal (February 2016), removal of the sludge layer may not have had the desired effect and there could be other hydrological issues within the MSB. For further uses and studies of MSBs, it is suggested that they are placed in areas where sedimentation is low or there is some barrier system in place to reduce weathering of surrounding rock. These barriers could be silt covers, vegetation covers, or anything that prevents high amounts of sediment from reaching the reactor. Closed or reclaimed mine sites would be the best uses for MSBs, due to cost effectiveness of the reactor and the likelihood of these sites having lower sediment loads. If a sludge layer still accumulates on these sites, it may need to be removed less often than on the current active site. Based on this study the sludge could then be stored in an anoxic environment to reduce the risk of further contamination.

### 4.3 References

- Chen L-X, Hu M, Huang L-N, et al (2014) Comparative metagenomic and metatranscriptomic analyses of microbial communities in acid mine drainage. *ISME J* 9:1579–1592. doi: 10.1038/ismej.2014.245
- DiLoreto ZA, Weber PA, Olds W, et al (2016) Novel cost effective full scale mussel shell bioreactors for metal removal and acid neutralization. *J Environ Manage.* doi: 10.1016/j.jenvman.2016.09.023
- McCauley CA, O’Sullivan AD, Milke MW, et al (2009) Sulfate and metal removal in bioreactors treating acid mine drainage dominated with iron and aluminum. *Water Res* 43:961–970. doi: 10.1016/j.watres.2008.11.029
- Trumm D, Ball J, Pope J, Weisener C (2015) Passive Treatment of ARD Using Mussel Shells – Part III : Technology Improvement and Future Direction. 10th Int Conference Acid Rock Drain IMWA Conf 1–9.
- Uster B, O’Sullivan AD, Ko SY, et al (2014) The Use of Mussel Shells in Upward-Flow Sulfate-Reducing Bioreactors Treating Acid Mine Drainage. *Mine Water Environ* 34:442–454. doi: 10.1007/s10230-014-0289-1

## APPENDIX

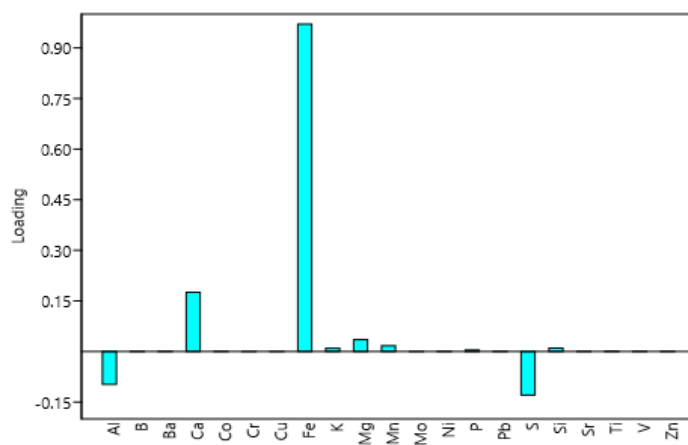
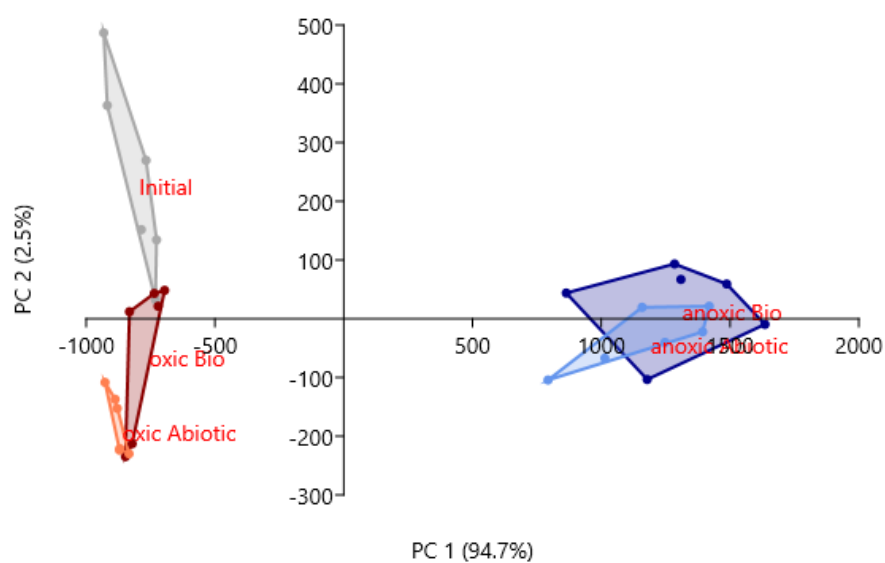


**Figure A 1** PCA of the bioavailable showing PC1 and PC1 (top) and the metal loadings (bottom) for the lab study (chapter 2).

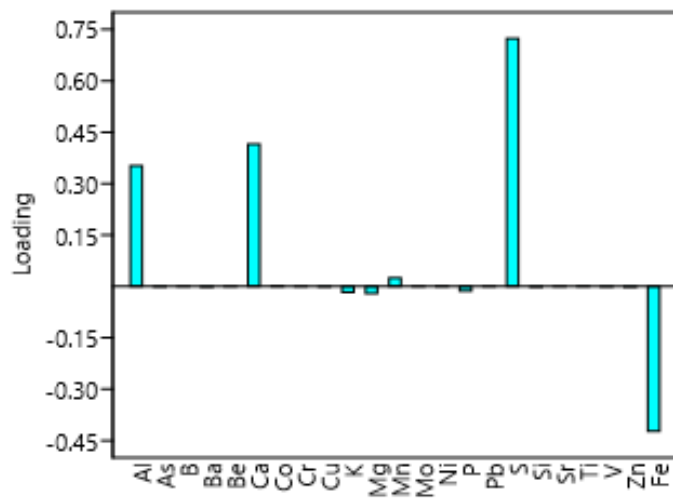
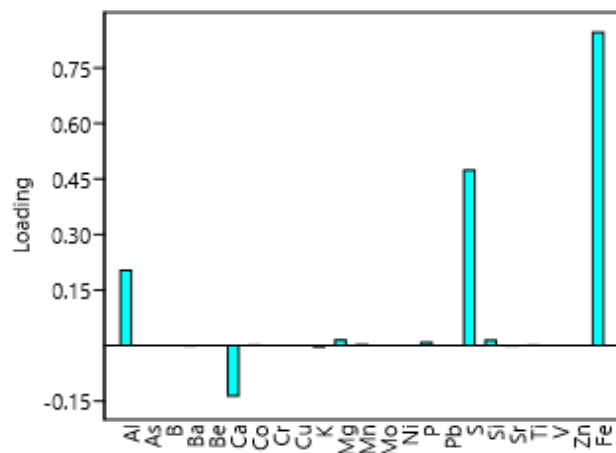


**Figure A 2** Oxyhydroxide loadings for PC1 (top) and PC2 (bottom) for the lab study (chapter 2).

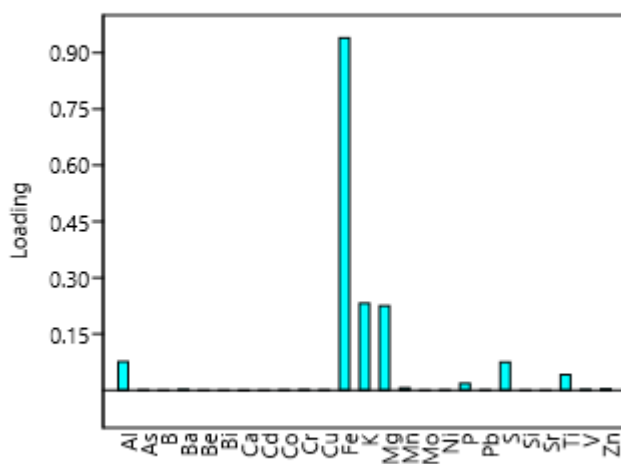
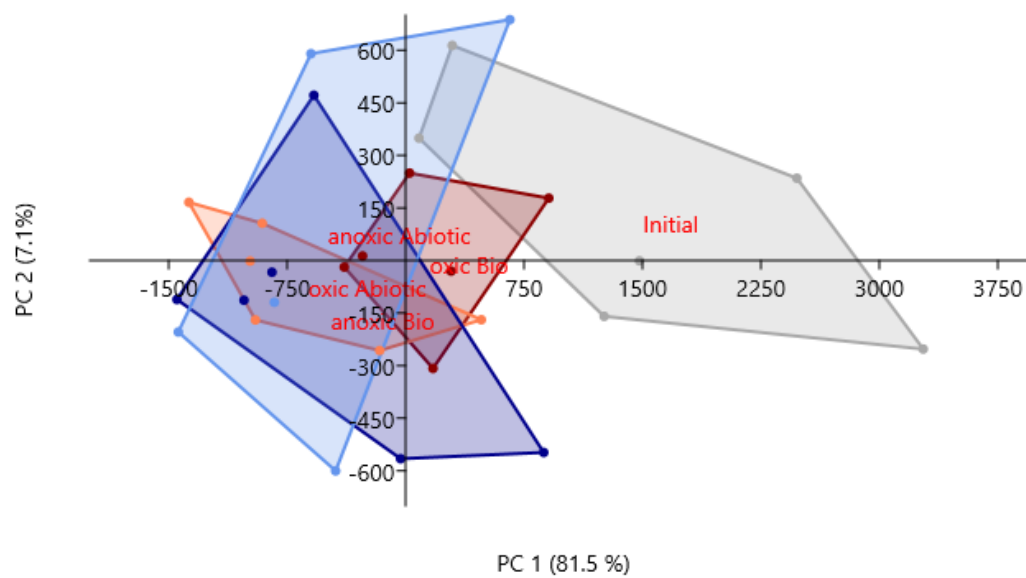


**Figure A 3** PCA of the Strong acid extractable showing PC1 and PC1 (top) and the metal loadings (bottom) for the lab study (chapter 2).



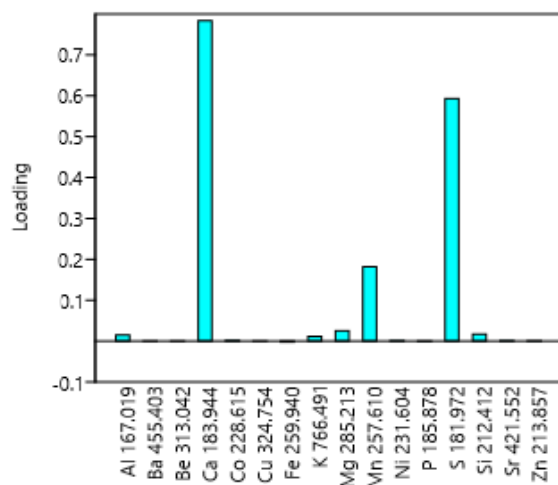
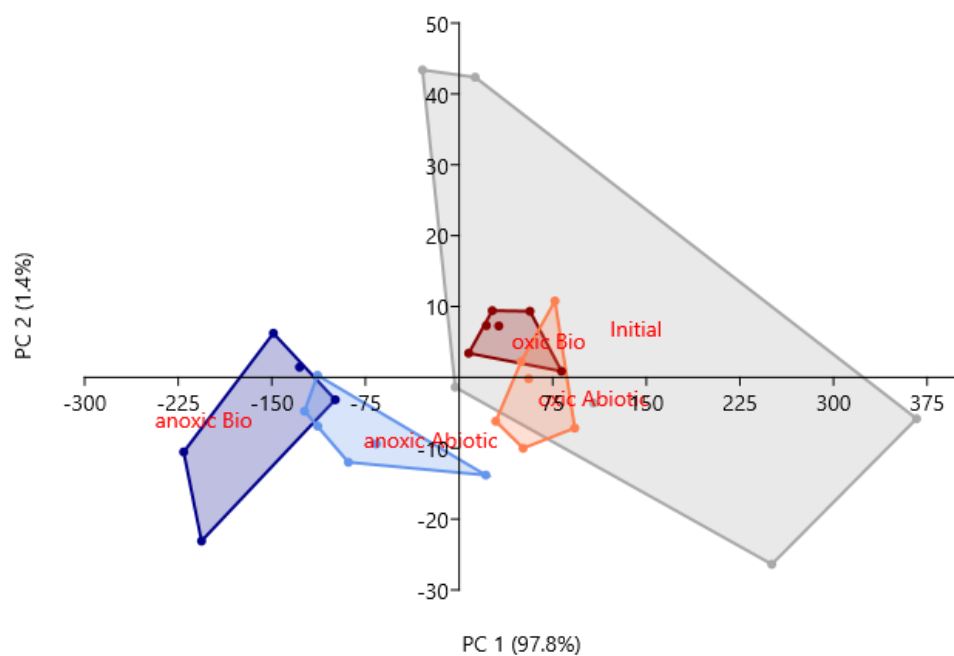


**Figure A 4** PCA of the water soluble phase showing PC1 and PC1 (top) and the metal loadings (bottom) for the lab study (chapter 2).

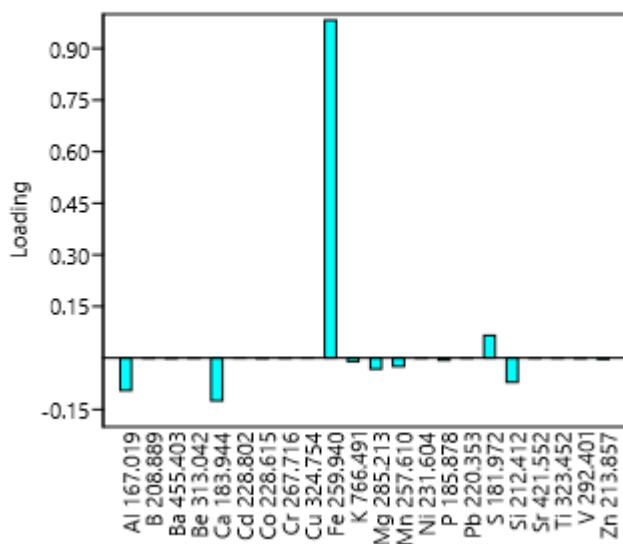
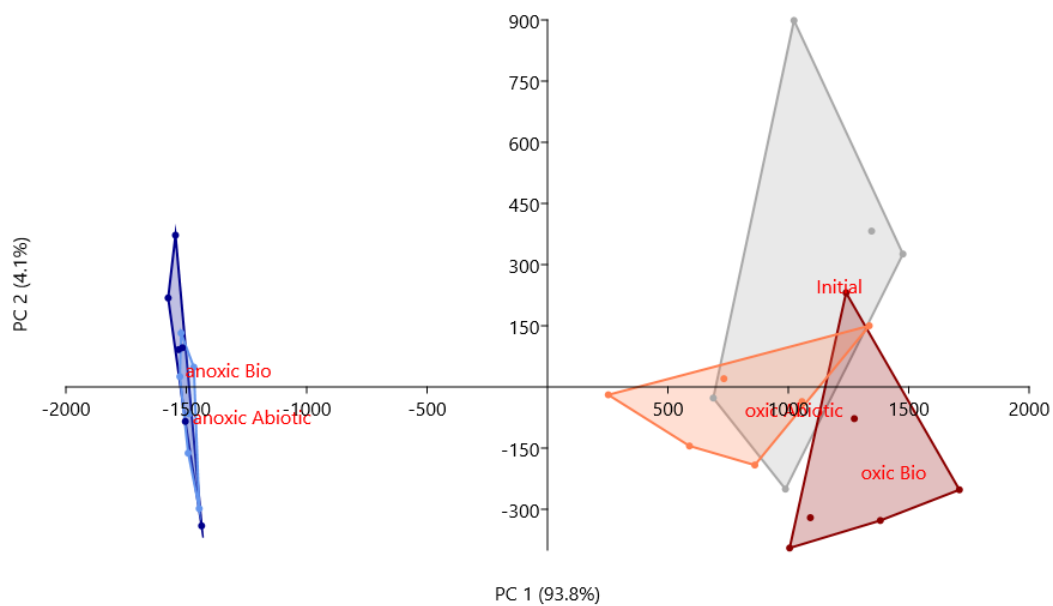


**Figure A 5** PCA of the weakly bound to oxide phase showing PC1 and PC1 (top) and the metal loadings (bottom) for the lab study (chapter 2).

**Table A 1** PC scores for each geochemical phase used in the CCA for the lab study (chapter 2).

	PC 1 Amorphous	PC 2 Amorphous	Bioavailable	Oxides	Water Soluble	Strong Acid
Initial	303.64	-544.05	-696.96	184.45	229.24	2828.8
Initial	138.26	-19.073	-673.37	950.76	86.127	2022
Initial	108.06	-462.21	-516.03	818.45	-24.784	848.55
Initial	131.8	-180.5	-516.23	438.6	344.89	1047.1
Initial	329.66	173.86	-459.97	577.57	-51.915	-161.77
Initial	14.041	-102.99	-460.26	498.74	-9.6555	-357.85
Oxic	39.919	133.29	-429.43	518.54	34.689	-710.45
Oxic	-4.5974	27.785	-470.89	890.87	60.175	450.22
Oxic	-103.24	224.54	-453.75	769.07	4.528	-242.55
Oxic	109.13	181	-564.71	602.56	9.8249	-159.35
Oxic	338.68	487.2	-564.05	720.78	-14.232	-820.41
Oxic	294.51	39.578	-540.05	1216.7	-0.1857	-420.08
Anoxic	-500.14	-115.26	1574.5	-2067.4	-227.43	-1062.4
Anoxic	-367.26	306.69	1589	-2002.8	-170.71	-1473.1
Anoxic	-433.68	-71.659	1768.9	-2026.3	-149.59	-488.01
Anoxic	-398.77	-78.214	1413.3	-2090.6	-120.98	-1300.7

**Table A 2** Geochemical bioavailable phase data showing average (Ave) and standard deviation (SD) for each incubation environment and the initial mg/L for the lab study (chapter 2).

<b>Bioavailable (mg/L)</b>		<b>Al</b>	<b>Ca</b>	<b>Fe</b>	<b>Mg</b>	<b>Mn</b>	<b>S</b>	<b>Zn</b>
<b>Initial</b>	<b>Ave</b>	461	292	210	6	75	358	1.1
	<b>SD</b>	3	25	63	1	10	30	0.4
<b>Oxic Bio</b>	<b>Ave</b>	360	299	211	8.7	51	414	0.7
	<b>SD</b>	20	19	66	0.3	6	42	0.4
<b>Oxic Abiotic</b>	<b>Ave</b>	125	357	91	11	85	114	1.5
	<b>SD</b>	22	60	17	2	34	88	0.3
<b>Anoxic Bio</b>	<b>Ave</b>	174	324	2242	7.4	49	424	0.6
	<b>SD</b>	39	49	240	0.5	4	35	0.2
<b>Anoxic Abiotic</b>	<b>Ave</b>	156	835	2079	115	96	187	1.6
	<b>SD</b>	13	45	225	11	15	21	0.1

**Table A 3** Geochemical oxyhydroxide phase data showing average (Ave) and standard deviation (SD) for each incubation environment and the initial in mg/L for the lab study (chapter 2).

<b>Oxyhydroxide</b>		<b>Al</b>	<b>Ca</b>	<b>Fe</b>	<b>Mg</b>	<b>Mn</b>	<b>S</b>	<b>Zn</b>
<b>Initial</b>	<b>Ave.</b>	348	879	1094	161	68	783	2.0
	<b>SD</b>	65	117	220	11	16	66	0.3
<b>oxic Bio</b>	<b>Ave.</b>	273	413	1592	169	39	732	1.4
	<b>SD</b>	98	60	165	34	4	120	0.4
<b>Oxic Abiotic</b>	<b>Ave.</b>	331	678	947	130	37	626	1.2
	<b>SD</b>	118	116	276	22	6	118	0.3
<b>Anoxic Bio</b>	<b>Ave.</b>	154	787	1048	161	46	233	1.0
	<b>SD</b>	66	229	359	22	22	46	0.2
<b>Anoxic Abiotic</b>	<b>Ave.</b>	107	571	559	161	46	299	1.1
	<b>SD</b>	27	156	88	32	10	46	0.2

**Table A 4** Geochemical strong acid extractable phase data showing average (Ave) and standard deviation (SD) for each incubation environment and the initial in mg/L for the lab study (chapter 2).

<b>Strong Acid</b>		<b>Al</b>	<b>Ca</b>	<b>Fe</b>	<b>Mg</b>	<b>Mn</b>	<b>S</b>	<b>Zn</b>
<b>Initial</b>	<b>Ave</b>	1343	826	9533	1740	157	679	33
	<b>SD</b>	211	184	909	222	27	74	4
<b>Oxic Bio</b>	<b>Ave</b>	1350	877	8014	1387	109	587	22
	<b>SD</b>	107	69	372	163	6	37	2
<b>Oxic Abiotic</b>	<b>Ave</b>	1182	802	7343	1127	106	737	21
	<b>SD</b>	67	56	629	101	6	81	2
<b>Anoxic Bio</b>	<b>Ave</b>	1427	1220	7402	1295	221	302	23
	<b>SD</b>	119	253	766	119	77	78	3
<b>Anoxic Abiotic</b>	<b>Ave</b>	1280	1114	7369	1517	197	315	28
	<b>SD</b>	120	297	523	577	33	62	7

**Table A 5** Geochemical water-soluble extractable phase data showing average (Ave) and standard deviation (SD) for each incubation environment and the initial in mg/L for the lab study (chapter 2).

<b>Water soluble</b>		<b>Al</b>	<b>Ca</b>	<b>Fe</b>	<b>Mg</b>	<b>Mn</b>	<b>S</b>	<b>Zn</b>
<b>Initial</b>	<b>Ave</b>	1.6	360	0	33	63	258	0.53
	<b>SD</b>	0.5	85	0	5	10	45	0.18
<b>Oxic Bio</b>	<b>Ave</b>	8.2	336	0	27	41	245	0.22
	<b>SD</b>	0.9	20	0	3	4	14	0.04
<b>Oxic Abiotic</b>	<b>Ave</b>	13.9	357	0	24	41	254	0.17
	<b>SD</b>	3.3	15	0	3	5	14	0.09
<b>Anoxic Bio</b>	<b>Ave</b>	1.6	182	0.5	23	7	105	0.24
	<b>SD</b>	0.6	33	0.6	3	5	40	0.19
<b>Anoxic Abiotic</b>	<b>Ave</b>	1.8	250	1.8	24	12	168	0.15
	<b>SD</b>	1.2	40	1.8	3	4	30	0.14

**Table A 6** Geochemical phases associated with weakly bound oxides data showing average (Ave) and standard deviation (SD) for each incubation environment and the initial in mg/L, for the lab study (chapter 2).

<b>Weak Acid</b>		<b>Al</b>	<b>Ca</b>	<b>Fe</b>	<b>Mg</b>	<b>Mn</b>	<b>S</b>	<b>Zn</b>
<b>Initial</b>	<b>Ave</b>	1223	1213	2557	285	151	625	10
	<b>SD</b>	141	204	291	44	44	51	5
<b>Oxic Bio</b>	<b>Ave</b>	748	1058	2721	289	68	577	17
	<b>SD</b>	169	90	225	28	11	113	4
<b>Oxic Abiotic</b>	<b>Ave</b>	1006	1027	1879	258	72	643	15
	<b>SD</b>	83	142	906	31	5	112	1
<b>Anoxic Bio</b>	<b>Ave</b>	1218	1495	0	385	167	484	5
	<b>SD</b>	185	169	0	53	66	118	1
<b>Anoxic Abiotic</b>	<b>Ave</b>	1172	1350	0	348	145	493	7
	<b>SD</b>	127	84	0	33	11	129	1



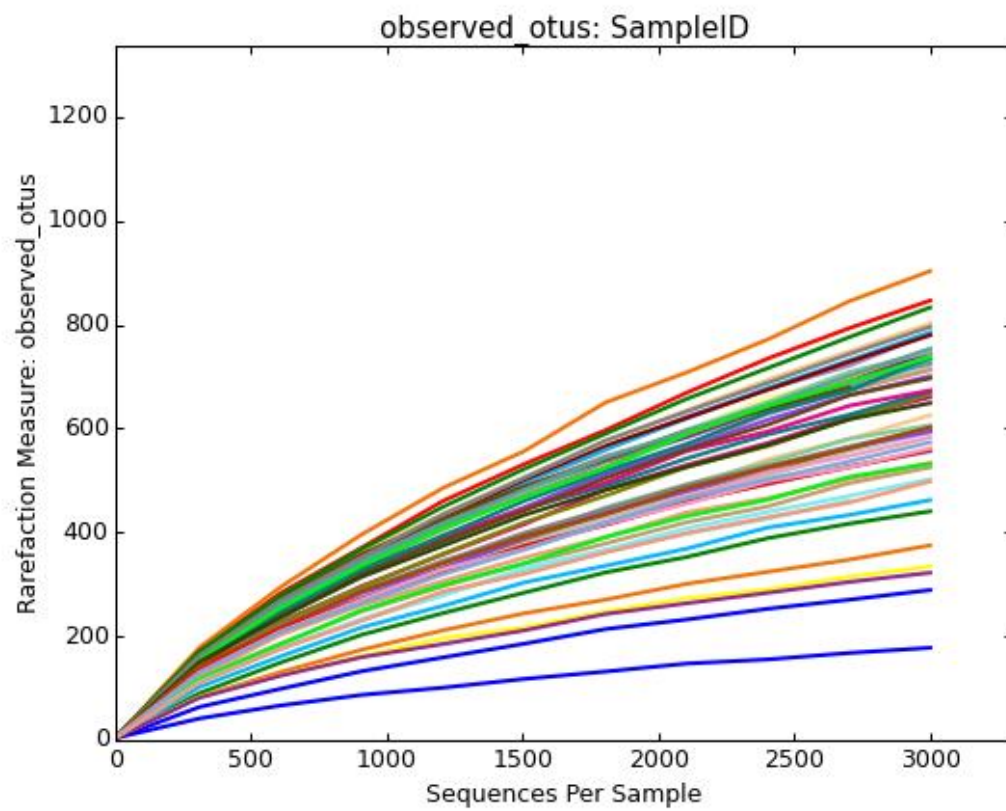


**Figure A 6** Rarefaction of each sample used in the analysis for the lab study (chapter 2).

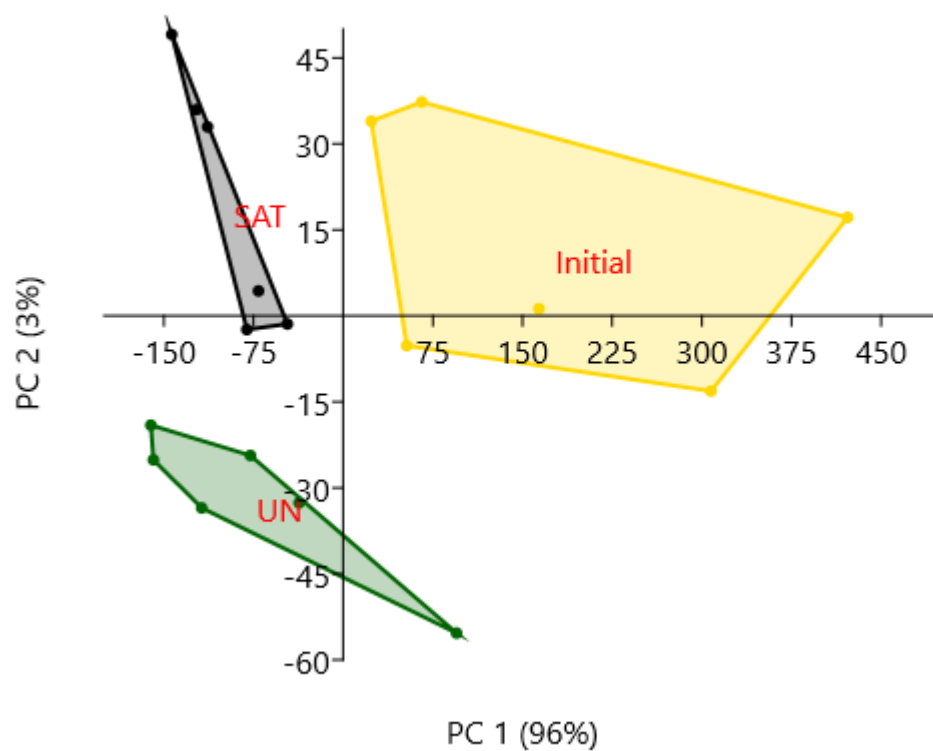


**Figure A 7** Water soluble phase extraction for the field column experiments. Green (UN) represents the unsaturated, yellow (Initial) is the initial sludge, and Black (SAT) are samples from the saturated column.

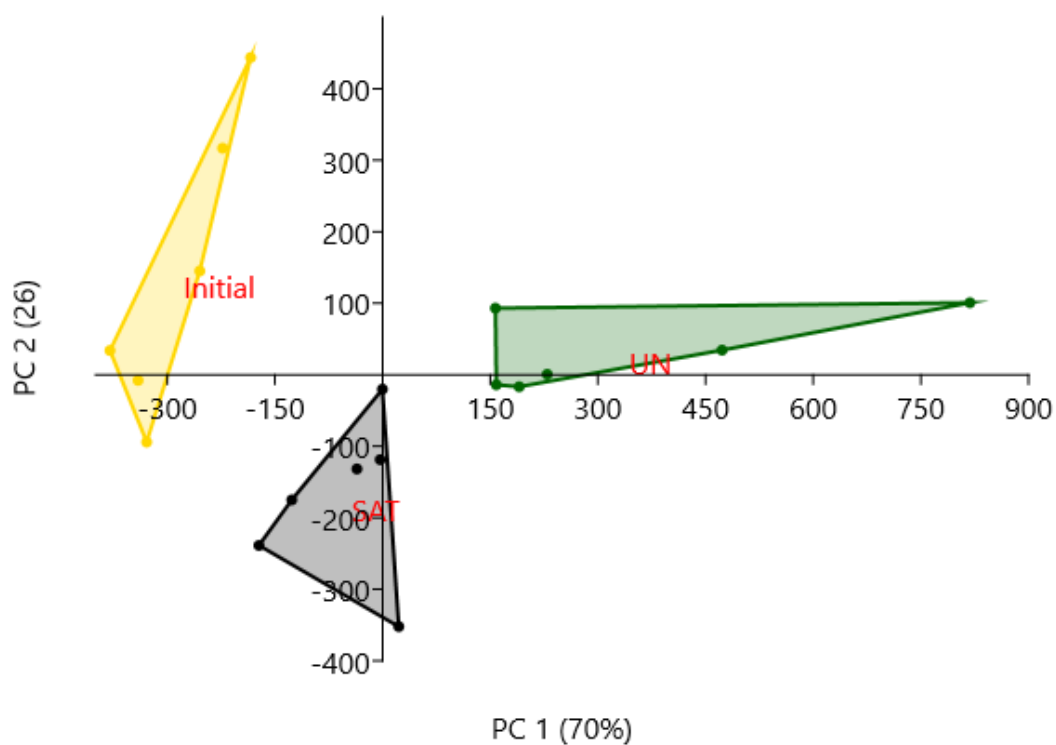


**Figure A 8** Bioavailable (associated with organic matter) phase extraction for the field column experiments. Green (UN) represents the unsaturated, yellow (Initial) is the initial sludge, and Black (SAT) are samples from the saturated column.

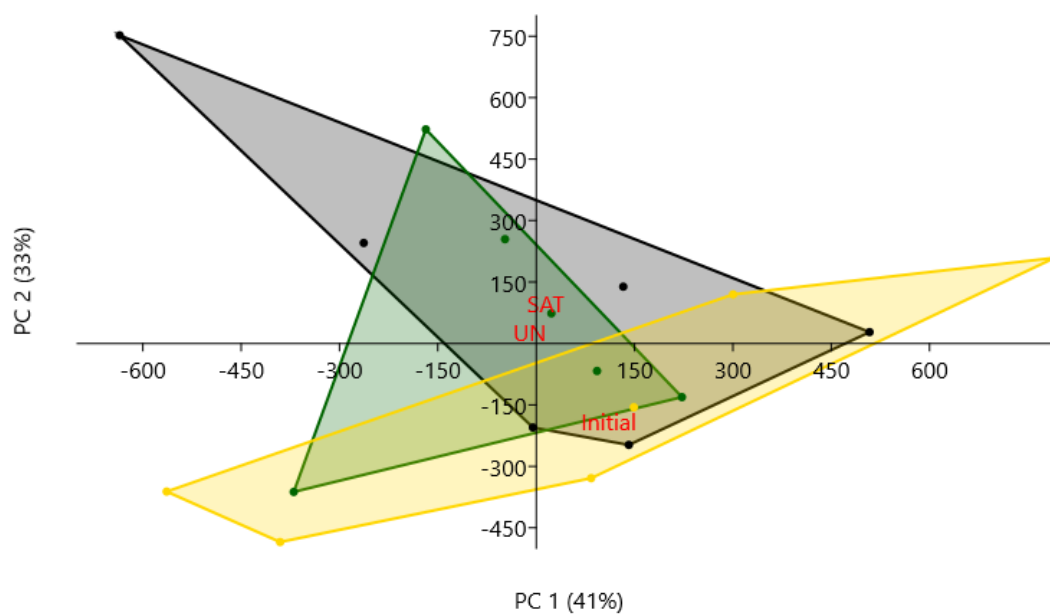


**Figure A 9** Oxyhydroxide phase extraction for the field column experiments. Green (UN) represents the unsaturated, yellow (Initial) is the initial sludge, and Black (SAT) are samples from the saturated column.

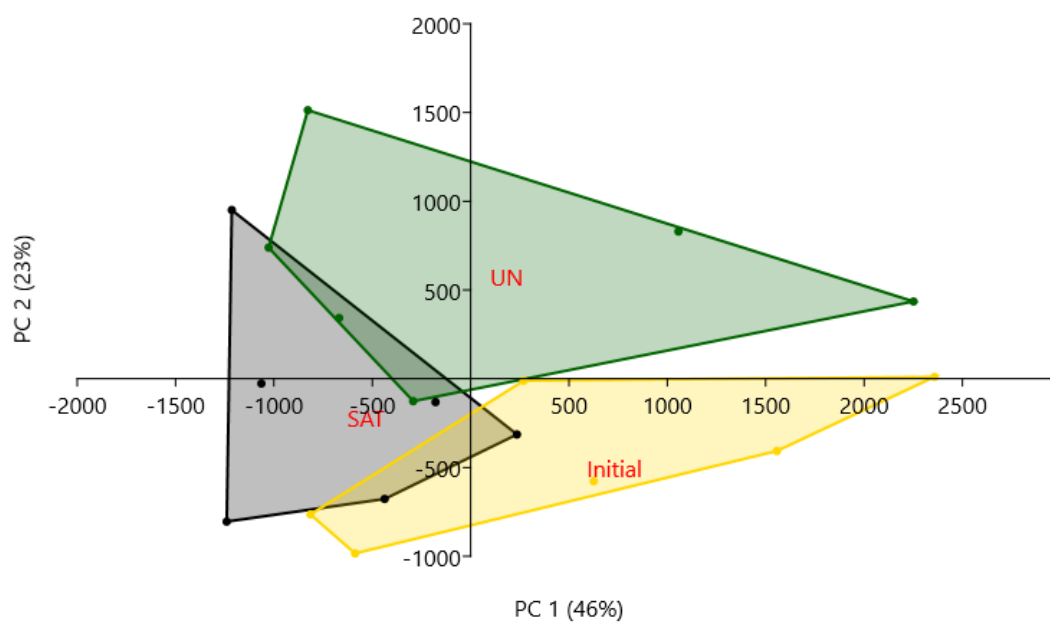


**Figure A 10** Strong acid extractable phase extraction for the field column experiments. Green (UN) represents the unsaturated, yellow (Initial) is the initial sludge, and Black (SAT) are samples from the saturated column.

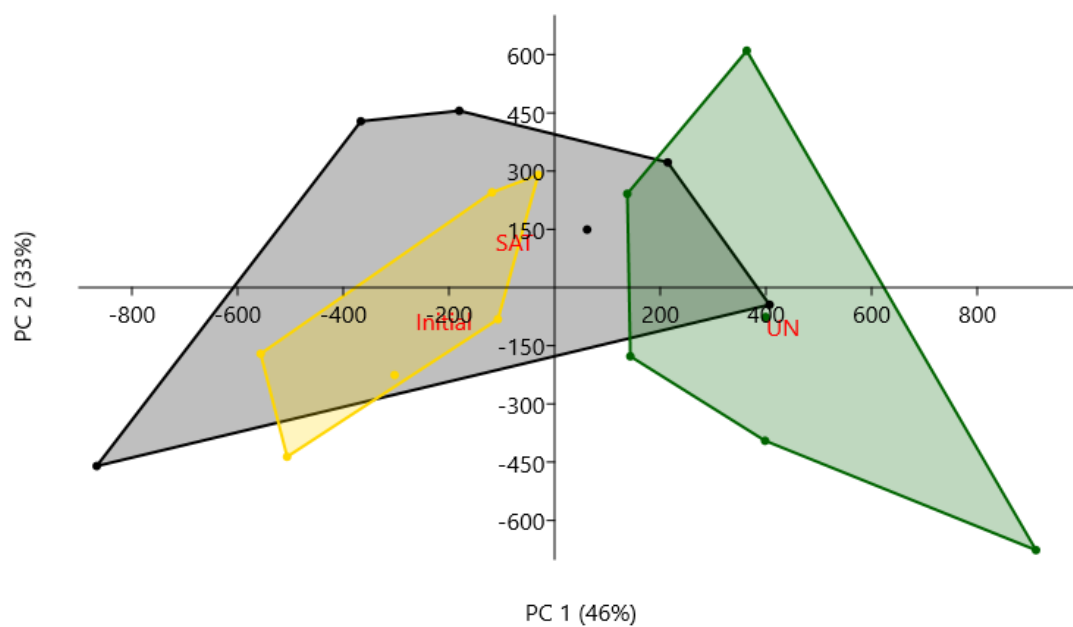


**Figure A 11** Metals weakly bound to iron oxides phase extraction for the field column experiments. Green (UN) represents the unsaturated, yellow (Initial) is the initial sludge, and Black (SAT) are samples from the saturated column.

## VITA AUCTORIS

NAME: Sara Butler

PLACE OF BIRTH: St. John's, NL

YEAR OF BIRTH: 1993

EDUCATION: Queen Elizabeth Regional High School,  
Conception Bay South, NL, 2011

Memorial University of Newfoundland and  
Labrador, B.Sc.(Hons), St. John's, NL, 2015